DMD Fast Forward. Published on June 23, 2021 as DOI: 10.1124/dmd.121.000430
This article has not been copyedited and formatted. The final version may differ from this version.

Title Page

Comparative hepatic and intestinal efflux transport of statins[#]

Feng Deng,[1] Suvi-Kukka Tuomi,[1] Mikko Neuvonen, Päivi Hirvensalo, Sami Kulju, Christoph Wenzel, Stefan Oswald, Anne M. Filppula, Mikko Niemi

Department of Clinical Pharmacology, Faculty of Medicine, University of Helsinki, Helsinki, Finland (F.D., S.K.T., M.Ne, P.H., S.K., A.M.F., M.Ni.)

Individualized Drug Therapy Research Program, Faculty of Medicine, University of Helsinki, Helsinki, Finland (F.D., S.K.T., M.Ne, P.H., S.K., A.M.F., M.Ni.)

Institute of Pharmacology, Center of Drug Absorption and Transport, University Medicine Greifswald, Greifswald, Germany (C.W., S.O.)

Institute of Pharmacology and Toxicology, Rostock University Medical Center, Rostock, Germany (S.O.)

Department of Clinical Pharmacology, HUS Diagnostic Center, Helsinki University Hospital, Helsinki, Finland (M.Ni.)

DMD Fast Forward. Published on June 23, 2021 as DOI: 10.1124/dmd.121.000430
This article has not been copyedited and formatted. The final version may differ from this version.

Running Title Page

Running title: Statin transport by efflux transporters

Corresponding author: Mikko Niemi, Department of Clinical Pharmacology, PO Box 20 (Tukholmankatu 8 C), 00014 University of Helsinki, Finland. Phone: +358 50 428 0998, Fax: +358 9471 74039, E-mail: mikko.niemi@helsinki.fi

Number of text pages: 18

Number of tables: 1

Number of figures: 7

Number of references: 54

Number of words in the Abstract: 249

Number of words in the Introduction: 510

Number of words in the Discussion: 1,658

Nonstandard abbreviations: ABC, ATP-binding cassette; AUC, area under the plasma concentration-time curve; BCRP, breast cancer resistance protein; BSEP, bile salt export pump, C_{max}, peak plasma concentration, CL, clearance; HEK, human embryonic kidney; HMG-CoA, 3-hydroxy-3-methylglutaryl coenzyme A; K_m, Michaelis-Menten constant; LC-MS/MS, liquid chromatography-tandem mass spectrometry; MRP, multidrug resistance-associated protein; OATP, organic anion transporting polypeptide; P-gp, P-glycoprotein; SCHH; sandwich-culture human hepatocyte; V_{max}, maximal transport rate.

DMD Fast Forward. Published on June 23, 2021 as DOI: 10.1124/dmd.121.000430
This article has not been copyedited and formatted. The final version may differ from this version.

Abstract

Previous studies have shown that lipid-lowering statins are transported by various ATP-binding cassette (ABC) transporters. However, due to varying methods, it is difficult to compare the transport profiles of statins. Therefore, we investigated the transport of ten statins or statin metabolites by six ABC transporters using human embryonic kidney cell-derived membrane vesicles. The transporter protein expression levels in the vesicles were quantified with liquid chromatography-tandem mass spectrometry, and used to scale the measured clearances to tissue levels. In our study, apically expressed breast cancer resistance protein (BCRP) and P-glycoprotein (P-gp) transported atorvastatin, fluvastatin, pitavastatin, and rosuvastatin. Multidrug resistance-associated protein 3 (MRP3) transported atorvastatin, fluvastatin, pitavastatin, and to a smaller extent, pravastatin. MRP4 transported fluvastatin and rosuvastatin. The scaled clearances suggest that BCRP contributes to 84-90% and 82% of the total active efflux of rosuvastatin in the small intestine and the liver, respectively. For atorvastatin, the corresponding values for P-gp-mediated efflux were 32-73% and 56%, respectively. MRP3, on the other hand, may contribute to 33-38% and 35-51% of total active efflux of atorvastatin, fluvastatin, and pitavastatin in jejunal enterocytes and liver hepatocytes, respectively. These data indicate that BCRP may play an important role in limiting the intestinal absorption and facilitating the biliary excretion of rosuvastatin and that P-gp may restrict the intestinal absorption and mediate the biliary excretion of atorvastatin. Moreover, the basolateral MRP3 may enhance the intestinal absorption and sinusoidal hepatic efflux of several statins. Taken together, the data show that statins differ considerably in their efflux transport profiles.

DMD Fast Forward. Published on June 23, 2021 as DOI: 10.1124/dmd.121.000430
This article has not been copyedited and formatted. The final version may differ from this version.

Significance Statement

This study characterized and compared the transport of atorvastatin, fluvastatin, pitavastatin, pravastatin, rosuvastatin, and simvastatin acid, and four atorvastatin metabolites by six ABC transporters (BCRP, MRP2, MRP3, MRP4, MRP8, P-gp). Based on *in vitro* findings and protein abundance data, we conclude that BCRP, MRP3 and P-gp have a major impact in the efflux of various statins. Together with *in vitro* metabolism, uptake transport and clinical data, our findings are applicable for use in comparative systems pharmacology modelling of statins.

DMD Fast Forward. Published on June 23, 2021 as DOI: 10.1124/dmd.121.000430
This article has not been copyedited and formatted. The final version may differ from this version.

Introduction

Cardiovascular diseases are among the most common causes of death, accounting for approximately 17.9 million deaths worldwide in 2015 (Roth *et al.*, 2017). 3-hydroxy-3-methylglutaryl coenzyme A (HMG-CoA) reductase inhibitors, also known as statins, are first-line drugs for primary and secondary prevention of cardiovascular diseases. Statins inhibit mevalonate production mediated by HMG-CoA reductase, which is a key step in cholesterol biosynthesis. Inhibition of this enzyme leads to a reduced cholesterol production and increased expression of low-density lipoprotein (LDL) cholesterol receptors in the liver (Slater and MacDonald, 1988). Ultimately, this results in a reduction in LDL cholesterol and triglyceride levels, accompanied by decreased mortality and coronary events (Maron *et al.*, 2000). Statins may also exert beneficial effects through a cholesterol-independent, pleiotropic manner by reducing systemic inflammation and platelet hyper-reactivity, and improving endothelial function (Liao and Laufs, 2005). While statins are widely used and generally accepted as efficient and safe (Yebyo *et al.*, 2019), they may cause muscle toxicity ranging from mild and relatively common myalgia to rare, but life-threatening rhabdomyolysis (Harper and Jacobson, 2007).

Drug transporters play a key role in regulating drug levels in systemic circulation and various tissues (Giacomini *et al.*, 2010). These proteins are located on the plasma membranes of cells, where they either pump their substrates into the cytosol or out of the cell. Adenosine triphosphate (ATP)-binding cassette (ABC) transporters are efflux pumps that utilize ATP to expel their substrates out of cells. Besides numerous drugs and other xenobiotics, they have an important task of excreting endogenous metabolites and waste products. P-glycoprotein (P-gp) and breast cancer resistance protein (BCRP) are amongst the most important efflux transporters, followed by bile salt export pump (BSEP) and multidrug resistance-associated protein 2 (MRP2) (Hillgren *et al.*, 2013). These transporters are abundantly expressed on the apical cell membranes in various pharmacokinetically relevant tissues such as the intestine, liver, kidney, and blood-brain barrier. There, they limit the absorption and promote the elimination of a wide range of compounds. In contrast, the efflux transporters MRP3 and MRP4 are located on the basolateral cell membranes in the intestine and liver. These transporters

DMD Fast Forward. Published on June 23, 2021 as DOI: 10.1124/dmd.121.000430
This article has not been copyedited and formatted. The final version may differ from this version.

pump their substrates towards systemic blood flow, thus promoting absorption and affecting the distribution of their substrates (Kitamura et al., 2010b; van de Wetering et al., 2009).

In general, the statins have limited oral bioavailabilities, due to marked first-pass loss (Neuvonen *et al.*, 2006; Elsby *et al.*, 2012). In the intestine, they are subject to biotransformation and apical efflux back to gut lumen. In the liver, they are extensively transported into hepatocytes by organic anion transporting polypeptides (OATP), which are important determinants of systemic exposure and clearance of the statins (Niemi *et al.*, 2011). However, statin transport by the efflux transporters located on basolateral membranes in the intestine and liver are less well characterized. Since these transporters may also regulate the intracellular statin concentrations, their role in statin pharmacokinetics should be investigated in more detail. Hence, the present study aimed to compare the transport of atorvastatin, atorvastatin metabolites, fluvastatin, pitavastatin, pravastatin, rosuvastatin, and simvastatin acid by different efflux transporters using a vesicular transport assay.

DMD Fast Forward. Published on June 23, 2021 as DOI: 10.1124/dmd.121.000430
This article has not been copyedited and formatted. The final version may differ from this version.

Materials and methods

Materials

Atorvastatin, atorvastatin-d5, 2-hydroxyatorvastatin, 2-hydroxyatorvastatin-d5, 2-hydroxyatorvastatin lactone, 2-hydroxyatorvastatin lactone-d5, 4-hydroxyatorvastatin, 4-hydroxyatorvastatin-d5, 4-hydroxyatorvastatin lactone, 4-hydroxyatorvastatin lactone-d5, fluvastatin-d8, pitavastatin-d5, pravastatin, pravastatin-d9, rosuvastatin, rosuvastatin-d6, and simvastatin acid-d6 were purchased from Toronto Research Chemicals (Toronto, Canada). Racemic fluvastatin, 3R,5S-fluvastatin, 3S,5R-fluvastatin, and pitavastatin were obtained from Santa Cruz Biotechnology (Dallas, Texas, USA). Simvastatin acid was purchased from SynFine Research (Ontario, Canada). Vesicles made of human embryonic kidney (HEK293) cells were purchased from PharmTox at the Radboud University Medical Center (PharmTox, Radboud UMC, Nijmegen, The Netherlands). Solvents used in assays and analytical methods were of analytical quality and purchased from Sigma-Aldrich (St. Louis, Missouri, USA). Ultrapure water for assays and analyses was purified using Milli-Q® water purification system (Merck Millipore, Burlington, Massachusetts, USA).

Vesicular transport assay

Vesicular transport assay was used to examine statin transport. The assays were performed essentially as described previously (Lehtisalo *et al.*, 2020). In brief, transporter-expressing membrane vesicles (7.5 µg) were pre-incubated at 37 °C for 10 minutes in transport assay buffer (PharmTox, Radboud UMC, Nijmegen, The Netherlands) supplemented with 10 mM $MgCl_2$ and various concentrations of statins. After the pre-incubation, the transport was started by adding pre-warmed Mg-ATP solution (final concentration 4 mM) or distilled water to the wells. Solvent concentration in the assays were not more than 1.0% in screening and time-dependent transport studies, and 1.5% in concentration-dependent transport studies. The reactions were incubated at 37 °C for desired time, after which the transport was terminated with 200 µL ice-cold stop buffer (PharmTox, Radboud UMC, Nijmegen, The Netherlands). Samples were then transferred onto a MultiScreenHTS FB Filter Plate 1.0 µm / 0.65 µm

DMD Fast Forward. Published on June 23, 2021 as DOI: 10.1124/dmd.121.000430
This article has not been copyedited and formatted. The final version may differ from this version.

(Merck KGaA, Darmstadt, Germany) and the vesicles were washed twice with 200 µL stop buffer and twice with ice-cold washing buffer (40 mM MOPS-Tris pH 7.0 and 70 mM KCl). After washing, the filter wells were air-dried, and the statins were eluted from vesicles with 50% methanol containing 25 ng/ml of isotope-labeled statin as an internal standard. All assays were performed in triplicates on 96-well plates.

Transport studies

The vesicular transport assay and the function of membrane vesicles were verified by investigating the transport of estradiol-17-glucuronide and N-methyl-quinidine, known MRP and P-gp substrates, respectively. Statin transport was initially screened in BCRP, MRP2, MRP3, MRP4, MRP8, P-gp and control vesicles. 10 µM of atorvastatin, 3R,5S-fluvastatin, 3S,5R-fluvastatin, pitavastatin, pravastatin and rosuvastatin, and 1 µM of simvastatin acid were incubated with the vesicles for 10 min. In addition, the transport of 10 µM atorvastatin metabolites was screened similarly in BCRP, MRP2, MRP3, MRP4, P-gp, and control vesicles. Parent statin-transporter combinations that exhibited notably higher uptake in the presence of ATP compared to that in the absence of ATP were further studied for time-linear range of transport with incubation times of 5, 10, and 15 minutes. Finally, the concentration-dependent transport (transporter kinetics) for confirmed substrates was determined in at least three separate experiments, where the statin concentration ranged from 6 to 200 µM. The incubation time (5 min) was selected based on the results of the time-dependency experiments. Racemic fluvastatin was employed in the kinetic studies, since the fluvastatin enantiomers exhibited no selectivity in the investigated transporters and racemic mixture was more readily available.

5’-nucleotidase activity assay.

The 5’-nucleotidase activity assay was used to determine the fraction of inverted membrane vesicles, essentially as described previously (Meszaros *et al.*, 2011). In short, 15 µg of transporter membrane

DMD Fast Forward. Published on June 23, 2021 as DOI: 10.1124/dmd.121.000430
This article has not been copyedited and formatted. The final version may differ from this version.

vesicles were incubated at 37 °C for 30 min with and without 3 mM AMP and 0.3% Triton X-100 in 50 mM Tris-HCl (pH 7.4), and 4 mM $MgCl_2$. The inorganic phosphate generated from AMP by 5′-nucleotidase located on the extracellular side of the plasma membrane was measured using Malachite Green Phosphate Detection Kit (R&D Systems, Minneapolis, Minnesota, USA).

The 5′-nucleotidase activity was determined at four conditions: A) measurement with AMP and Triton X-100, which provides the maximum activity; B) measurement with AMP only, which provides the activity in right-side-out vesicles; C) measurement with Triton X-100 only, which shows the phosphate background in the presence of Triton X-100; D) measurement without AMP and Triton X-100, which shows the background phosphate in the assay buffer.

Equation 1: $$f_{inverted} = \frac{(A-C)-(B-D)}{A-C} * 100\%$$

The fraction of inverted membrane vesicles was calculated using the equation 1. In the equation, A, B, C, and D indicate the amount of inorganic phosphate at the four conditions described above. A-C describes the total activity of 5'-nucleotidase, whereas B-D describes the activity of 5'-nucleotidase in the right-side-out vesicles.

Analytical methods

All statins and statin metabolites were analyzed using a Sciex 5500 Qtrap LC-MS/MS system (AB Sciex, Framingham, Massachusetts, USA) interfaced with an ESI ion source. The chromatographic separation was performed on a Luna Omega polar C18 analytical column (100x2.1mm I.D., 1.6µm particle size; Phenomenex, Torrance, California, USA) protected by a guard column of the same material. The mobile phase A and B consisted of 5 mM ammonium formate (pH 3.9, adjusted with 98% formic acid) and acetonitrile, respectively, and the flow rate and the column temperature were maintained at 300 µL/min and 40 ˚C. The following gradient conditions were applied: 1 min at 20% B on hold, then a linear ramp from 20% B to 40% B over 3 min followed by a second linear ramp to

DMD Fast Forward. Published on June 23, 2021 as DOI: 10.1124/dmd.121.000430
This article has not been copyedited and formatted. The final version may differ from this version.

90% B over 2 min, and 1 min at 90% B before a re-equilibration step back to the initial conditions (20% B). The mass spectrometer was operated in multiple reaction monitoring (MRM) mode and the characteristic ion transitions for each analyte and internal standard are presented in Supplementary Table S1.

Protein amounts (pmol/mg of protein) of BCRP, MRP2, MRP3, MRP4, and P-gp in vesicles were quantified by mass spectrometry-based targeted proteomics using a validated LC−MS/MS method as described elsewhere (Gröer *et al.*, 2013; Oswald *et al.*, 2019). The isolated vesicles were subjected to determination of the whole protein concentrations using the bicinchoninic acid (BCA) assay (Thermo Fisher Scientific, Schwerte, Germany). If necessary, membrane fractions were adjusted to a maximum protein amount of 2 mg/mL. Subsequently, the membrane vesicles were directly digested with trypsin without further processing. In brief, 100 µL of each membrane fraction were mixed with 10 µL dithiothreitol (200 mM, Sigma-Aldrich, Taufkirchen, Germany), 40 µL ammonium bicarbonate buffer (50 mM, pH 7.8, Sigma-Aldrich), and 10 µL ProteaseMAX (1%, m/v, Promega, Mannheim, Germany) and incubated for 20 min at 60 °C. After cooling down, 10 µL iodoacetamide (400 mM, Sigma-Aldrich) were added and the samples were incubated in a darkened water bath for 15 min at 37 °C. For protein digestion, 10 µL trypsin (trypsin/protein ratio: 1/40, Promega) was added and samples were incubated in a water bath for 16 h at 37 °C. Digestion was stopped by addition of 20 µL formic acid (10% v/v, Sigma-Aldrich). Afterwards, the samples were centrifuged one more time for 15 min at 16,000 g and 4 °C. 50 µL of the supernatant were mixed with 25 µL isotope-labeled internal standard peptide mix (10 nM of each labeled peptide, Thermo Fisher Scientific). All sample preparation and digestion steps were performed using Protein LoBind tubes (Eppendorf, Hamburg, Germany). Protein quantification was conducted on a 5500 QTRAP triple quadrupole mass spectrometer (AB Sciex, Darmstadt, Germany) coupled to an Agilent Technologies 1260 Infinity system (Agilent Technologies, Waldbronn, Germany). Transporter proteins were simultaneously quantified using proteospecific peptides. Final protein abundance data (picomoles per milligram) were calculated by normalization to the total protein content of the isolated membrane fraction as determined by the BCA assay.

DMD Fast Forward. Published on June 23, 2021 as DOI: 10.1124/dmd.121.000430
This article has not been copyedited and formatted. The final version may differ from this version.

Data and statistical analysis

ATP-dependent transport was calculated by subtracting the statin uptake into vesicles in the absence of ATP from the statin uptake into vesicles in the presence of ATP. Uptake ratio was determined by uptake of investigated statin into vesicles in the presence of ATP divided to that in the absence of ATP. The ATP-dependent transport and uptake ratios in screening and time-dependent transport studies were compared to those in control vesicles using one-way analysis of variance (ANOVA) and Fisher's Least Significant Difference analysis (GraphPad Software version 8.4, San Diego, California, USA). A P value below 0.05 was considered statistically significant.

The kinetic parameters of statin transport were determined with GraphPad Prism 8.4. For these calculations, the mean ATP-dependent transport values of each concentration point from separate experiments were pooled, and these values were fitted to the Michaelis-Menten equation (Equation 2), where v stands for the velocity of ATP-dependent transport, V_{max} for the maximal transport rate, [S] for the substrate concentration and K_m for the Michaelis-Menten constant.

$$\text{Equation 2:} \qquad v = \frac{V_{max}\,[S]}{K_m + [S]}$$

The *in vitro* statin clearance was calculated from Michaelis-Menten parameters as shown in Equation 3.

$$\text{Equation 3:} \qquad CL_{in\ vitro} = \frac{V_{max}}{K_m}$$

The *in vitro* statin clearance was adjusted with vesicle protein expression as shown in Equation 4,

$$\text{Equation 4:} \qquad CL_{adj} = \frac{CL_{in\ vitro}}{Protein\ expression_{in\ vitro} * f_{inverted}}$$

where CL_{adj} stands for expression-adjusted clearance, Protein $expression_{in\ vitro}$ for transporter abundance measured in vesicles, and $f_{inverted}$ for the fraction of membrane vesicles that is inverted

DMD Fast Forward. Published on June 23, 2021 as DOI: 10.1124/dmd.121.000430
This article has not been copyedited and formatted. The final version may differ from this version.

(0.333, from Keppler et al., 1998). The clearance was further scaled to the tissue level by multiplying CL_{adj} with published transporter abundance data (Equation 5).

Equation 5: $$CL_{tissue} = CL_{adj} * Protein\ expression_{tissue}$$

In the Equation 5, CL_{tissue} is the estimated tissue level efflux statin clearance, and Protein $expression_{tissue}$ is the abundance of the efflux transporter in the tissue of interest (Burt *et al.*, 2016; Drozdzik *et al.*, 2019).

DMD Fast Forward. Published on June 23, 2021 as DOI: 10.1124/dmd.121.000430
This article has not been copyedited and formatted. The final version may differ from this version.

Results

Transport of known substrates of MRP2, MRP3, MRP4, MRP8, and P-gp

The functionalities of the vesicles were verified using estradiol-17-glucuronide (50 µM for MRP2; 10 µM for MRP3, MRP4, MRP8, and control vesicles) and N-methyl-quinidine (5 µM for P-gp) as positive controls. The uptake ratios of these probe substrates in MRP2, MRP3, MRP4, MRP8, and P-gp vesicles were 79, 38, 15, 2.8, and 2.4, respectively, verifying the functionality of the vesicles and vesicular transport assay (Supplementary figure S1).

Screening of statin efflux transport

The screening of statin transport was conducted by incubating 10 µM of statins (or 1 µM in the case of simvastatin acid) with BCRP, MRP2, MRP3, MRP4, MRP8, P-gp, and control vesicles (Figure 1, Supplementary table S2). Atorvastatin was significantly transported by MRP3 (uptake ratio 2.2 ± 0.6), and P-gp (3.1 ± 0.6), and the uptake ratio of transport differed significantly from control (MRP3, $P = 0.0102$; P-gp, $P < 0.0001$). 3R,5S-fluvastatin was significantly transported by BCRP (3.8 ± 0.9, $P < 0.0001$) and P-gp (2.8 ± 0.3, $P = 0.0078$), while 3S,5R-fluvastatin was significantly transported by BCRP (3.1 ± 1.6, $P = 0.0497$), MRP3 (3.2 ± 1.0, $P = 0.0261$), and MRP4 (3.1 ± 0.8, $P = 0.0458$). Pitavastatin was clearly transported by BCRP (4.6 ± 0.6, $P = 0.0006$) and P-gp (3.3 ± 1.0, $P = 0.0306$), and rosuvastatin was efficiently transported by BCRP (8.4 ± 3.1, $P = 0.0002$). For pravastatin and simvastatin acid, none of the uptake ratios differed significantly from the control.

In addition, we tested the transport of 10 µM atorvastatin metabolites; 2-hydroxyatorvastatin, 4-hydroxyatorvastatin, 2-hydroxyatorvastatin lactone, and 4-hydroxyatorvastatin lactone in BCRP, MRP2, MRP3, MRP4, P-gp, and control vesicles. 2-hydroxyatorvastatin was taken up in BCRP (uptake ratio 3.5 ± 0.9, $P = 0.0279$) and MRP3 (3.3 ± 0.6, $P = 0.0492$) vesicles significantly more than in control vesicles (uptake ratio 1.9 ± 0.7) (Figure 1, Supplementary table S3). The transport of 4-

DMD Fast Forward. Published on June 23, 2021 as DOI: 10.1124/dmd.121.000430
This article has not been copyedited and formatted. The final version may differ from this version.

hydroxyatorvastatin in MRP3 (4.4 ± 1.5, P = 0.0028) and P-gp (4.0 ± 1.1, P = 0.0076) vesicles differed significantly from control vesicles (1.3 ± 0.7). The 2- and 4-hydroxyatorvastatin lactones showed no transport in any vesicles (Supplementary table S3).

Time-dependent transport

The transport of statins by selected transporters were further investigated by studying the time-dependent transport (Supplementary figures S2-S7, Supplementary tables S4-S5). In most cases, when notable transport was observed, the ATP-dependent transport plateaued already at 5 min as the statin uptake into vesicles and the escape of the statins due to passive diffusion reached equilibrium.

Atorvastatin transport was already prominent at 5 min in BCRP, MRP3, and P-gp vesicles with uptake ratios of 2.5 (P = 0.0012), 2.2 (P = 0.0167), and 2.5 (P = 0.0019), respectively, which were significantly higher than that in control vesicles (Supplementary figure S2). On the other hand, the ATP-dependent transport and uptake ratio in MRP2 and MRP4 vesicles did not differ from the control vesicles, except for MRP2 at 10 min time-point.

The transport rates of both fluvastatin enantiomers in BCRP, MRP3, and P-gp vesicles were significantly higher than those in control vesicles at any given time, and the ATP-dependent transport was nearly plateaued 5 min after initiation of transport (Supplementary figures S3-S4). The 3R,5S-fluvastatin transport rate in MRP2 and MRP4 vesicles was higher than that in control vesicles at 5 and 10 min. The 3S,5R-fluvastatin transport rate in MRP2 and MRP4 vesicles was higher than that in control vesicles only at 10 min. The transport rates of 3R,5S-fluvastatin and 3S,5R-fluvastatin in MRP8 vesicles differed significantly from those of control vesicles only at 5 and 10 min time-points, respectively.

Pitavastatin was transported by BCRP with high efficiency: The transport rates in BCRP vesicles were three times higher than those in MRP3 and P-gp vesicles (Supplementary figure S5). The transport rates in MRP3 vesicles were significantly higher than those of control at 5 and 15 min time-points, but only at 15 min the uptake ratio of 2.3 was significantly greater than in control vesicles (P = 0.0011). P-

DMD Fast Forward. Published on June 23, 2021 as DOI: 10.1124/dmd.121.000430
This article has not been copyedited and formatted. The final version may differ from this version.

gp vesicles showed significantly higher transport rate (P = 0.0002), and the uptake ratio (3.6, P = 0.0004) at 5 min time-point than control vesicles.

In the screening, the uptake ratios of pravastatin were relatively high in BCRP, MRP3, and MRP4 vesicles, although they did not differ significantly from that of control vesicles. For this reason, the time-dependent transport of pravastatin was further studied. MRP3 exhibited low, yet significant transport rates at 5 min (P = 0.0050) and 15 min (P = 0.0115) time-points despite notable variation (Supplementary figure S6). In addition, the uptake ratio at 5 min (2.2, P = 0.0018) was significantly greater than that of control. Pravastatin transport rates in BCRP, MRP2, and MRP4 vesicles did not differ significantly from control, except for MRP2 at 15 min (P = 0.0473).

Rosuvastatin was transported by BCRP with high rate and uptake ratio at any given time, although the ATP-dependent transport plateaued already at 5 min (Supplementary figure S7). While the MRP4 and P-gp transported rosuvastatin to some extent, the transport rates did not differ significantly from control vesicles, and were approximately an order of magnitude lower than those in BCRP vesicles. Only the transport rate at 10 min in MRP4 vesicles was significantly greater than that in control vesicles (P = 0.0410). The high uptake ratio of rosuvastatin in MRP8 vesicles in screening studies was not replicated in the time-dependency studies.

The time-dependent transport of simvastatin acid was not further investigated, as the uptake ratios of simvastatin acid transport in the screening were relatively close to that in control vesicles.

Concentration-dependent transport (transporter kinetics)

Based on atorvastatin screening and time-dependency studies, BCRP, MRP3, and P-gp were selected for kinetic measurements (Figure 2). Atorvastatin had apparent affinities of 82.4, 31.5, and 10.7 μM, in BCRP, MRP3 and P-gp, respectively (Table 1). The maximum transport rate in the investigated transporters followed the same order, the rate being the greatest for BCRP and the lowest for P-gp.

DMD Fast Forward. Published on June 23, 2021 as DOI: 10.1124/dmd.121.000430
This article has not been copyedited and formatted. The final version may differ from this version.

Racemic fluvastatin was employed in kinetic studies, since the enantiomers exhibited no distinct selectivity in the investigated transporters and racemic mixture is more readily available. Racemic fluvastatin was well-transported by BCRP and MRP3 with similarly high affinities (K_m 25.8 and 48.9 µM, respectively), although the transport rate in BCRP was three times higher than that in MRP3 (Table 1, Figure 3). In addition, MRP2, MRP4, MRP8, and P-gp vesicles were also capable of accumulating racemic fluvastatin in a concentration-dependent manner. Large deviation was observed in experiments despite the numerous replications, and this reflects to the reliability of estimated Michaelis-Menten parameters. Therefore, only the curve fit and parameters of BCRP can be considered reliable. Nevertheless, the ATP-dependent transport was notably lower in control vesicles than in other vesicles. Furthermore, the uptake ratio in three control experiments was on average 1.26 ± 0.15, whereas the uptake ratio of MRP2 and P-gp, which had lowest ratio and highest deviation, respectively, were 1.81 ± 0.44 and 2.39 ± 1.09 (Supplementary table S6).

The apparent affinities of pitavastatin in BCRP, MRP3 and P-gp vesicles were high and relatively similar across the transporters (16, 9.0, and 37 µM, respectively, Figure 4). The maximum rate of transport in BCRP vesicles was four times higher than in others vesicles (Table 1). The MRP3-mediated transport of pitavastatin was less clear as the uptake ratio of 12 µM pitavastatin in MRP3 vesicles remained below two (1.8 ± 0.2).

Pravastatin was transported in MRP3 vesicles only (Figure 5). In the kinetic studies, pravastatin transport exhibited non-saturable transport over the concentration range. Furthermore, the clearance of pravastatin was notably lower compared to the clearance of other statins in MRP3 (Table 1).

Rosuvastatin is a well-established BCRP substrate with high transport rate and apparent affinity of transport. This was confirmed in our study with a single experiment, which concluded that K_m of rosuvastatin transport in BCRP was approximately 4.2 µM (Figure 6). Meanwhile the apparent affinities of rosuvastatin in MRP4 and P-gp vesicles were 10-fold lower (K_m of 39.3 and 46.2 µM, respectively). However, their transport rates in the presence of high concentrations of rosuvastatin showed large variability, which leads to the unreliable estimation of Michaelis-Menten parameters.

DMD Fast Forward. Published on June 23, 2021 as DOI: 10.1124/dmd.121.000430
This article has not been copyedited and formatted. The final version may differ from this version.

5’-nucleotidase activity and the fraction of inverted membrane vesicles

The fraction of inverted membrane vesicles was determined using the 5’-nucleotidase activity assay (Supplementary figure S8). The $f_{inverted}$ of BCRP, MRP2, MRP4, MRP8, and P-gp vesicles were similar (36-52%), whereas the $f_{inverted}$ of MRP3 vesicles was higher (65%).

Proteomic measurements of membrane vesicles and the estimation of tissue-specific active efflux clearance

The transporter abundance in vesicle preparations was measured with a quantitative proteomic technique based on LC-MS/MS. The absolute abundances in BCRP, MRP2, MRP3, MRP4, and P-gp vesicles were 146, 85, 54, 44, and 59 pmol/mg of protein, respectively (Supplementary table S7).

Based on the *in vitro* results, 5’-nucleotidase activity data, proteomics measurements, and published transporter abundance data from literature, we calculated the expression-adjusted clearance, $CL_{adj,}$ (Table 1), and the individual contribution of efflux transporters to the total active efflux clearance in various tissues (Figure 7, Supplementary table S8). For atorvastatin, fluvastatin, and pitavastatin, basolateral pumps were estimated to contribute to approximately 50% and 25% of their efflux clearance in duodenal and jejunal enterocytes, respectively. While the contribution of these transporters diminishes in the ileum, it still remains notable (approximately 15%). Similarly in the hepatocytes, basolateral efflux, primarily mediated by MRP3, was estimated to contribute to more than one third of the total known hepatic efflux of these statins. The scaled efflux clearance estimation underlines the impact of BCRP in rosuvastatin efflux, where over 84% of efflux clearance, in both the intestine and liver, was estimated to be mediated by BCRP. For atorvastatin, P-gp was estimated to comprise nearly 90% of its apical efflux clearance. Its role is particularly evident in the liver, where P-gp is much more abundant than BCRP.

DMD Fast Forward. Published on June 23, 2021 as DOI: 10.1124/dmd.121.000430
This article has not been copyedited and formatted. The final version may differ from this version.

Discussion

In the present study, we evaluated the transport of six statins by six efflux transporters relevant for drug absorption, distribution, and elimination. This study is unique in that the transport was studied using uniform methods in a single laboratory, thus allowing comparison of statin efflux profiles. Of the apical efflux transporters tested, BCRP and P-gp transported atorvastatin, fluvastatin, pitavastatin, and rosuvastatin, and MRP2 transported fluvastatin. Interestingly, atorvastatin, fluvastatin, pitavastatin, and pravastatin were transported by the basolaterally expressed MRP3, and fluvastatin and rosuvastatin by MRP4. Simvastatin acid was not transported by any of the investigated transporters. This could be due to high passive permeability, which may result in a false negative result in the vesicular transport assay. Furthermore, kinetic parameters from membrane vesicle assays combined with protein expression data, allowed the scaling of the obtained findings to tissue level. Taken together, our data indicate that statins differ in their efflux transport profiles.

BCRP, MRP2, and P-gp are expressed on the apical plasma membranes in tissues important for pharmacokinetics. There, they limit the absorption and facilitate the excretion of their substrates. Previous pharmacogenetic studies have suggested that BCRP restricts the intestinal absorption of atorvastatin, fluvastatin, and rosuvastatin (Keskitalo, Pasanen, *et al.*, 2009; Keskitalo, Zolk, *et al.*, 2009). Indeed, we observed extensive BCRP-mediated transport of fluvastatin, pitavastatin, and rosuvastatin, and minor, but significant transport of atorvastatin. The more lipophilic pitavastatin and especially atorvastatin were good P-gp substrates, whereas the hydrophilic rosuvastatin was poorly transported by P-gp. Interestingly, all the statins transported by P-gp contain at least one nitrogen atom, which could be beneficial when interacting with the negatively charged binding cavity of P-gp (Deng *et al.*, 2020).

MRP3 and MRP4 are expressed on the basolateral plasma membrane in small intestine and liver (Drozdzik *et al.*, 2019). According to a recent meta-analysis, the hepatic abundance of MRP3 in healthy Caucasian adults is similar to that of P-gp and 40% lower than that of MRP2 (Burt et al. 2016). Furthermore, when all the ethnicities and disease states were included in the meta-analysis, the hepatic abundance of MRP4 was 70% lower than that of MRP3 and similar to the level of BCRP. In

DMD Fast Forward. Published on June 23, 2021 as DOI: 10.1124/dmd.121.000430
This article has not been copyedited and formatted. The final version may differ from this version.

the enterocytes, they may facilitate the vectorial movement of their substrate drugs and metabolites by flipping them from the enterocyte to mesenteric blood (van de Wetering *et al.*, 2009; Kitamura *et al.*, 2010b; Proctor *et al.*, 2016). Our estimations of active efflux clearance suggests that this basolateral pathway may be important for the absorption of several statins (Figure 7). In the liver, statins are actively taken into the hepatocytes by OATP1B1, OATP1B3, and/or OATP2B1 (Bi *et al.*, 2019). MRP3 and MRP4 may partly counteract this by returning statins from hepatocytes back to the sinusoidal blood. We hypothesize that basolateral transporters may additionally promote statin elimination and pharmacological activity by distributing statins and their metabolites more evenly in the hepatocytes along the sinusoids. This hepatocyte hopping could prevent the saturation of the pharmacological target, metabolic enzymes, and biliary efflux transporters (Iusuf *et al.*, 2012). Based on our scaled clearance values, MRP3 could affect the intracellular statin efflux and enable hepatocyte shuffle for statins.

Atorvastatin is a lipophilic statin with an oral bioavailability of 14%, which is explained by first-pass hepatic extraction (Lennernäs, 2003). Here, the transport kinetics of atorvastatin and its metabolites were determined for the first time using membrane vesicles. The highest affinity and abundance-scaled clearance of atorvastatin were observed in P-gp vesicles. The estimated tissue-specific efflux clearances indicate that P-gp, and BCRP to a smaller extent, could regulate atorvastatin plasma and tissue levels in humans. In line with this, previous studies have demonstrated increased systemic exposure to atorvastatin in association with genetic variants, which reduce the function or expression of the P-gp and BCRP (Keskitalo *et al.*, 2008; Keskitalo, Zolk, *et al.*, 2009; León-Cachón *et al.*, 2016). Moreover, our findings suggest that MRP3 may facilitate the intestinal absorption of atorvastatin especially in the jejunum, and the hepatocyte hopping of atorvastatin and its metabolites. Moreover, MRP3 could be an important basolateral pathway for 2-hydroxyatorvastatin, which is extensively formed in the liver (Lau *et al.*, 2006).

Fluvastatin is a relatively lipophilic statin, but has a low bioavailability of 29%, partly due to extensive first-pass hepatic metabolism (Tse *et al.*, 1992). In the kinetic experiments, the highest transport rate and affinity were observed in BCRP vesicles, whereas the lowest affinity was seen in P-gp vesicles.

DMD Fast Forward. Published on June 23, 2021 as DOI: 10.1124/dmd.121.000430
This article has not been copyedited and formatted. The final version may differ from this version.

We also demonstrated for the first time that fluvastatin is transported in MRP2, MRP3, MRP4, and MRP8 vesicles. Our scaled efflux clearance values suggest that the BCRP plays a major role in the apical efflux of fluvastatin in the intestine, while both MRP2 and BCRP may be important for the biliary clearance. In humans, a reduced-function genetic variant of BCRP was associated with increased exposure to fluvastatin (Keskitalo, Pasanen, *et al.*, 2009). Furthermore, rat data supports a role for MRP2 in fluvastatin biliary excretion (Lindahl *et al.*, 2004), although observations in preclinical species must be treated with caution. Based on the scaled tissue efflux clearances, MRP3 and MRP4 could promote the intestinal absorption of fluvastatin. Together, MRP3 and MRP4 constitute 22-53% of the total intestinal efflux clearance, depending on the site along the small intestine. In the hepatocytes, MRP3 and MRP4 may account for over 31% of the total efflux clearance, and could thus enable fluvastatin hepatocyte hopping. Interestingly, fluvastatin was the sole substrate for MRP8 in our study. However, the impact of MRP8 remains elusive, since its membrane localization, abundance and function are poorly characterized.

Pitavastatin is a lipophilic and metabolically stable statin that undergoes enterohepatic circulation, which explains its relatively high bioavailability of 51% and long half-life of 13 h (Livalo Labeling-Package Insert., 2009; Saito, 2011). In the present study, BCRP and MRP3 transported pitavastatin with a similar affinity and scaled clearance, followed by P-gp with twofold lower affinity and clearance. Thus, we estimate that BCRP may comprise the majority of intestinal apical efflux, whereas BCRP and P-gp are equally important in its biliary clearance in hepatocytes. These estimations agree with the mechanistic modeling of pitavastatin disposition in sandwich-cultured human hepatocytes (SCHH) (Vildhede *et al.*, 2016). However, despite being a good BCRP substrate *in vitro* (Fujino *et al.*, 2005; Hirano, Maeda, Matsushima, *et al.*, 2005), the pharmacokinetics of pitavastatin has not been affected by genetic variants of BCRP (Ieiri *et al.*, 2007; Oh *et al.*, 2013; Zhou *et al.*, 2013). By contrast, a genetic variant of P-gp has been associated with increased C_{max} and AUC of pitavastatin (Zhou *et al.*, 2013). The scaled MRP3-mediated efflux clearance exceeded that of BCRP by twofold in the liver and was equal in jejunum. This agrees with data from the earlier SCHH study (Vildhede *et al.*, 2016). Therefore, MRP3 could facilitate pitavastatin absorption. In a previous study, the

accumulation of pitavastatin into the liver was reduced in Mrp2-deficient rats (Hirano, Maeda, Matsushima, *et al.*, 2005). Interestingly, the expression of Mrp3 is induced in these rats, supporting the importance of Mrp3 in the intrahepatic distribution of pitavastatin (Ogawa *et al.*, 2000; Kuroda *et al.*, 2004).

Pravastatin is a hydrophilic statin with a low bioavailability (18%), limited by acid-catalyzed biotransformation (Singhvi *et al.*, 1990) and hepatic uptake (Niemi et al., 2006). This is the first study to demonstrate that pravastatin is a substrate of MRP3. In fact, MRP3 was the only transporter, which transported pravastatin in our study. Our data may explain how pravastatin is transferred from enterocytes to the mesenteric vein, and effluxed from hepatocytes back to the circulation. Surprisingly, we observed no pravastatin transport in either HEK-MRP2 or Sf9-MRP2 vesicles (Supplementary figure S9), even though previous studies have suggested that MRP2 is a key canalicular transporter for pravastatin (Niemi, Arnold, *et al.*, 2006; Nakagomi-Hagihara *et al.*, 2007; Elsby *et al.*, 2011). In Mrp2-deficient rats, pravastatin C_{max} and AUC were increased compared to wild-type rats (Kivistö *et al.*, 2005), which might be explained by the increased hepatic Mrp3 expression. Instead of MRP2, BSEP could mediate the biliary excretion of pravastatin (Hirano, Maeda, Hayashi, *et al.*, 2005).

Rosuvastatin is another hydrophilic statin with a low bioavailability (20%), minimal metabolism, and a long terminal half-life of 20 h (Neuvonen *et al.*, 2006). Of the statins tested in our study, BCRP transported rosuvastatin with the highest affinity and clearance. In contrast, minimal transport of rosuvastatin was observed in P-gp and MRP4 vesicles. Our findings suggesting an important role for BCRP in the hepatic and intestinal efflux of rosuvastatin are consistent with clinical data showing over twofold increase in the C_{max} and AUC of rosuvastatin in healthy volunteers homozygous for a genetic defect in BCRP (Keskitalo, Zolk, *et al.*, 2009). The scaled clearance values imply that P-gp plays a limited role in rosuvastatin efflux, a finding supported by clinical pharmacogenetic data (Keskitalo, Kurkinen, *et al.*, 2009; Bai *et al.*, 2019). Due to its hydrophilic nature, rosuvastatin may require basolateral efflux transporters in absorption and distribution. MRP4 could facilitate rosuvastatin absorption in the duodenum, where it was estimated to contribute 10% of rosuvastatin efflux clearance. Rat liver perfusion and SCHH studies have demonstrated significant basolateral efflux of

DMD Fast Forward. Published on June 23, 2021 as DOI: 10.1124/dmd.121.000430
This article has not been copyedited and formatted. The final version may differ from this version.

rosuvastatin in the liver (Pfeifer, Bridges, *et al.*, 2013; Pfeifer, Yang, *et al.*, 2013), but in our estimations, the role of hepatic MRP4 was minimal due to low *in vitro* activity and hepatic expression (Burt *et al.*, 2016).

In conclusion, we compared the transport of atorvastatin, fluvastatin, pitavastatin, pravastatin, rosuvastatin, and simvastatin acid in BCRP, MRP2, MRP3, MRP4, MRP8, and P-gp vesicles. Using the vesicular transport assay and LC-MS/MS-based protein abundance measurements, we demonstrated the different efflux transport profiles and estimated the efflux clearances of statins in small intestine and liver. Due to assay variability in kinetic studies for certain statins and transporters, the estimated relative contributions of the different transporters to tissue efflux clearance should be interpreted with caution. Moreover, polarized-cell-monolayer-based or other alternative methods may be useful to confirm our findings. Overall, the present data can be applied to physiologically-based pharmacokinetic or systems pharmacology modelling of statins.

DMD Fast Forward. Published on June 23, 2021 as DOI: 10.1124/dmd.121.000430
This article has not been copyedited and formatted. The final version may differ from this version.

Acknowledgements

We would like to thank Dr. Erkka Järvinen, Dr. Moshe Finel, and Dr. Heidi Kidron for providing the Sf9 vesicles.

[#] This work was supported by the ERC Consolidator Grant (Grant Agreement number 725249).

DMD Fast Forward. Published on June 23, 2021 as DOI: 10.1124/dmd.121.000430
This article has not been copyedited and formatted. The final version may differ from this version.

Authorship Contributions

Participated in research design: Deng, Tuomi, Hirvensalo, and Niemi

Conducted experiments: Deng, Tuomi, Neuvonen, Kulju, Wenzel, and Oswald

Contributed new reagents or analytic tools: Neuvonen

Performed data analysis: Deng, Tuomi, Oswald, and Niemi

Wrote or contributed to the writing of the manuscript: Deng, Tuomi, Neuvonen, Hirvensalo, Kulju, Wenzel, Oswald, Filppula, and Niemi

DMD Fast Forward. Published on June 23, 2021 as DOI: 10.1124/dmd.121.000430
This article has not been copyedited and formatted. The final version may differ from this version.

References

Bai X, Zhang B, Wang P, Wang G, Li J, Wen D, Long X, Sun H, Liu Y, Huang M, and Zhong S (2019) Effects of SLCO1B1 and GATM gene variants on rosuvastatin-induced myopathy are unrelated to high plasma exposure of rosuvastatin and its metabolites. *Acta Pharmacol Sin* **40**:492–499.

Bi Y, Costales C, Mathialagan S, West M, Eatemadpour S, Lazzaro S, Tylaska L, Scialis R, Zhang H, Umland J, Kimoto E, Tess DA, Feng B, Tremaine LM, Varma MVS, and Rodrigues AD (2019) Quantitative Contribution of Six Major Transporters to the Hepatic Uptake of Drugs: "SLC-Phenotyping" Using Primary Human Hepatocytes. *J Pharmacol Exp Ther* **370**:72–83.

Burt HJ, Riedmaier AE, Harwood MD, Crewe HK, Gill KL, and Neuhoff S (2016) Abundance of Hepatic Transporters in Caucasians: A Meta-Analysis. *Drug Metab Dispos* **44**:1550–1561.

Deng F, Ghemtio L, Grazhdankin E, Wipf P, Xhaard H, and Kidron H (2020) Binding Site Interactions of Modulators of Breast Cancer Resistance Protein, Multidrug Resistance-Associated Protein 2, and P-Glycoprotein Activity. *Mol Pharm* **17**:2398–2410.

Drozdzik M, Busch D, Lapczuk J, Müller J, Ostrowski M, Kurzawski M, and Oswald S (2019) Protein Abundance of Clinically Relevant Drug Transporters in the Human Liver and Intestine: A Comparative Analysis in Paired Tissue Specimens. *Clin Pharmacol Ther* **105**:1204–1212.

Elsby R, Hilgendorf C, and Fenner K (2012) Understanding the Critical Disposition Pathways of Statins to Assess Drug–Drug Interaction Risk During Drug Development: It's Not Just About OATP1B1. *Clin Pharmacol Ther* **92**:584–598.

Elsby R, Smith V, Fox L, Stresser D, Butters C, Sharma P, and Surry DD (2011) Validation of membrane vesicle-based breast cancer resistance protein and multidrug resistance protein 2 assays to assess drug transport and the potential for drug–drug interaction to support regulatory submissions. *Xenobiotica* **41**:764–783.

Fujino H, Saito T, Ogawa S, and Kojima J (2005) Transporter-mediated influx and efflux mechanisms of pitavastatin, a new inhibitor of HMG-CoA reductase. *J Pharm Pharmacol* **57**:1305–1311.

Giacomini KM, Huang SM, Tweedie DJ, and et al. (2010) The International Transporter Consortium: Membrane transporters in drug development. *Nat Rev Drug Discov* **9**:215–236.

Gröer C, Brück S, Lai Y, Paulick A, Busemann A, Heidecke CD, Siegmund W, and Oswald S (2013) LC–MS/MS-based quantification of clinically relevant intestinal uptake and efflux transporter proteins. *J Pharm Biomed Anal* **85**:253–261.

Harper CR, and Jacobson TA (2007) The broad spectrum of statin myopathy: from myalgia to rhabdomyolysis: *Curr Opin Lipidol* **18**:401–408.

Hillgren KM, Keppler D, Zur AA, Giacomini KM, Stieger B, Cass CE, and Zhang L (2013) Emerging Transporters of Clinical Importance: An Update From the International Transporter Consortium. *Clin Pharmacol Ther* **94**:52–63.

Hirano M, Maeda K, Hayashi H, Kusuhara H, and Sugiyama Y (2005) Bile Salt Export Pump (BSEP/ABCB11) Can Transport a Nonbile Acid Substrate, Pravastatin. *J Pharmacol Exp Ther* **314**:876–882.

Hirano M, Maeda K, Matsushima S, Nozaki Y, Kusuhara H, and Sugiyama Y (2005) Involvement of BCRP (ABCG2) in the Biliary Excretion of Pitavastatin. *Mol Pharmacol* **68**:800–807.

Ieiri I, Suwannakul S, Maeda K, Uchimaru H, Hashimoto K, Kimura M, Fujino H, Hirano M, Kusuhara H, Irie S, Higuchi S, and Sugiyama Y (2007) SLCO1B1 (OATP1B1, an Uptake Transporter) and ABCG2 (BCRP, an Efflux Transporter) Variant Alleles and Pharmacokinetics of Pitavastatin in Healthy Volunteers. *Clin Pharmacol Ther* **82**:541–547.

Iusuf D, van de Steeg E, and Schinkel AH (2012) Hepatocyte Hopping of OATP1B Substrates Contributes to Efficient Hepatic Detoxification. *Clin Pharmacol Ther* **92**:559–562.

Keppler D, Jedlitschky G, and Leier I (1998) Transport function and substrate specificity of multidrug resistance protein, in *Methods in Enzymology* pp 607–616, Elsevier.

Keskitalo JE, Kurkinen KJ, Neuvonen M, Backman JT, Neuvonen PJ, and Niemi M (2009) No significant effect of *ABCB1* haplotypes on the pharmacokinetics of fluvastatin, pravastatin, lovastatin, and rosuvastatin. *Br J Clin Pharmacol* **68**:207–213.

Keskitalo JE, Kurkinen KJ, Neuvonen PJ, and Niemi M (2008) ABCB1 Haplotypes Differentially Affect the Pharmacokinetics of the Acid and Lactone Forms of Simvastatin and Atorvastatin. *Clin Pharmacol Ther* **84**:457–461.

Keskitalo JE, Pasanen MK, Neuvonen PJ, and Niemi M (2009) Different effects of the *ABCG2* c.421C>A SNP on the pharmacokinetics of fluvastatin, pravastatin and simvastatin. *Pharmacogenomics* **10**:1617–1624.

Keskitalo JE, Zolk O, Fromm MF, Kurkinen KJ, Neuvonen PJ, and Niemi M (2009) ABCG2 Polymorphism Markedly Affects the Pharmacokinetics of Atorvastatin and Rosuvastatin. *Clin Pharmacol Ther* **86**:197–203.

Kitamura Y, Kusuhara H, and Sugiyama Y (2010a) Basolateral Efflux Mediated by Multidrug Resistance-Associated Protein 3 (Mrp3/Abcc3) Facilitates Intestinal Absorption of Folates in Mouse. *Pharm Res* **27**:665–672.

Kitamura Y, Kusuhara H, and Sugiyama Y (2010b) Functional Characterization of Multidrug Resistance-Associated Protein 3 (Mrp3/ *Abcc3*) in the Basolateral Efflux of Glucuronide Conjugates in the Mouse Small Intestine. *J Pharmacol Exp Ther* **332**:659–666.

Kivistö KT, Grisk O, Hofmann U, Meissner K, Möritz K-U, Ritter C, Arnold KA, Lutjöohann D, von Bergmann K, Klöting I, Eichelbaum M, and Kroemer HK (2005) DISPOSITION OF ORAL AND INTRAVENOUS PRAVASTATIN IN MRP2-DEFICIENT TR ⁻ RATS. *Drug Metab Dispos* **33**:1593–1596.

Kuroda M, Kobayashi Y, Tanaka Y, Itani T, Mifuji R, Araki J, Kaito M, and Adachi Y (2004) Increased hepatic and renal expressions of multidrug resistance-associated protein 3 in Eisai hyperbilirubinuria rats. *J Gastroenterol Hepatol* **19**:146–153.

Lau YY, Okochi H, Huang Y, and Benet LZ (2006) Pharmacokinetics of atorvastatin and its hydroxy metabolites in rats and the effects of concomitant rifampicin single doses: relevance of first-pass effect from hepatic uptake transporters, and intestinal and hepatic metabolism. *Drug Metab Dispos* **34**:1175–1181.

Lehtisalo M, Keskitalo JE, Tornio A, Lapatto-Reiniluoto O, Deng F, Jaatinen T, Viinamäki J, Neuvonen M, Backman JT, and Niemi M (2020) Febuxostat, But Not Allopurinol, Markedly Raises the Plasma Concentrations of the Breast Cancer Resistance Protein Substrate Rosuvastatin. *Clin Transl Sci* **13**:1236–1243.

Lennernäs H (2003) Clinical pharmacokinetics of atorvastatin. *Clin Pharmacokinet* **42**:1141–1160.

León-Cachón RBR, Ascacio-Martínez JA, Gamino-Peña ME, Cerda-Flores RM, Meester I, Gallardo-Blanco HL, Gómez-Silva M, Piñeyro-Garza E, and Barrera-Saldaña HA (2016) A pharmacogenetic pilot study reveals MTHFR, DRD3, and MDR1 polymorphisms as biomarker candidates for slow atorvastatin metabolizers. *BMC Cancer* **16**:74.

Liao JK, and Laufs U (2005) Pleiotropic effects of statins. *Annu Rev Pharmacol Toxicol* **45**:89–118.

Lindahl A, Sjöberg Å, Bredberg U, Toreson H, Ungell A-L, and Lennernäs H (2004) Regional Intestinal Absorption and Biliary Excretion of Fluvastatin in the Rat: Possible Involvement of mrp2. *Mol Pharm* **1**:347–356.

Livalo Labeling-Package Insert. (2009) . *Kowa Pharm Am Inc*.

Maron DJ, Fazio S, and Linton MF (2000) Current perspectives on statins. *Circulation* **101**:207–213.

Meszaros P, Klappe K, Hummel I, Hoekstra D, and Kok JW (2011) Function of MRP1/ABCC1 is not dependent on cholesterol or cholesterol-stabilized lipid rafts. *Biochem J* **437**:483–491.

Nakagomi-Hagihara R, Nakai D, Tokui T, Abe T, and Ikeda T (2007) Gemfibrozil and its glucuronide inhibit the hepatic uptake of pravastatin mediated by OATP1B1. *Xenobiotica* **37**:474–486.

Neuvonen PJ, Niemi M, and Backman JT (2006) Drug interactions with lipid-lowering drugs: mechanisms and clinical relevance. *Clin Pharmacol Ther* **80**:565–581.

Niemi M, Arnold KA, Backman JT, Pasanen MK, Gödtel-Armbrust U, Wojnowski L, Zanger UM, Neuvonen PJ, Eichelbaum M, Kivistö KT, and Lang T (2006) Association of genetic polymorphism in ABCC2 with hepatic multidrug resistance-associated protein 2 expression and pravastatin pharmacokinetics: *Pharmacogenet Genomics* **16**:801–808.

Niemi M, Pasanen M, and Neuvonen P (2006) SLCO1B1 polymorphism and sex affect the pharmacokinetics of pravastatin but not fluvastatin. *Clin Pharmacol Ther* **80**:356–366.

Niemi M, Pasanen MK, and Neuvonen PJ (2011) Organic anion transporting polypeptide 1B1: a genetically polymorphic transporter of major importance for hepatic drug uptake. *Pharmacol Rev* **63**:157–181.

Ogawa K, Suzuki H, Hirohashi T, Ishikawa T, Meier PJ, Hirose K, Akizawa T, Yoshioka M, and Sugiyama Y (2000) Characterization of inducible nature of MRP3 in rat liver. *Am J Physiol-Gastrointest Liver Physiol* **278**:G438–G446.

Oh ES, Kim CO, Cho SK, Park MS, and Chung J-Y (2013) Impact of ABCC2, ABCG2 and SLCO1B1 Polymorphisms on the Pharmacokinetics of Pitavastatin in Humans. *Drug Metab Pharmacokinet* **28**:196–202.

Oswald S, Müller J, Neugebauer U, Schröter R, Herrmann E, Pavenstädt H, and Ciarimboli G (2019) Protein Abundance of Clinically Relevant Drug Transporters in The Human Kidneys. *Int J Mol Sci* **20**:5303.

Pfeifer ND, Bridges AS, Ferslew BC, Hardwick RN, and Brouwer KLR (2013) Hepatic Basolateral Efflux Contributes Significantly to Rosuvastatin Disposition II: Characterization of Hepatic Elimination by Basolateral, Biliary, and Metabolic Clearance Pathways in Rat Isolated Perfused Liver. *J Pharmacol Exp Ther* **347**:737–745.

Pfeifer ND, Yang K, and Brouwer KLR (2013) Hepatic Basolateral Efflux Contributes Significantly to Rosuvastatin Disposition I: Characterization of Basolateral Versus Biliary Clearance Using a Novel Protocol in Sandwich-Cultured Hepatocytes. *J Pharmacol Exp Ther* **347**:727–736.

Proctor WR, Ming X, Bourdet D, Han T (Kevin), Everett RS, and Thakker DR (2016) Why Does the Intestine Lack Basolateral Efflux Transporters for Cationic Compounds? A Provocative Hypothesis. *J Pharm Sci* **105**:484–496.

Roth GA, Johnson C, Abajobir A, Abd-Allah F, Abera SF, Abyu G, Ahmed M, Aksut B, Alam T, Alam K, Alla F, Alvis-Guzman N, Amrock S, Ansari H, Ärnlöv J, Asayesh H, Atey TM, Avila-Burgos L, Awasthi A, Banerjee A, Barac A, Bärnighausen T, Barregard L, Bedi N, Belay Ketema E, Bennett D, Berhe G, Bhutta Z, Bitew S, Carapetis J, Carrero JJ, Malta DC, Castañeda-Orjuela CA, Castillo-Rivas J, Catalá-López F, Choi J-Y, Christensen H, Cirillo M, Cooper L, Criqui M, Cundiff D, Damasceno A, Dandona L, Dandona R, Davletov K, Dharmaratne S, Dorairaj P, Dubey M, Ehrenkranz R, El Sayed Zaki M, Faraon EJA, Esteghamati A, Farid T, Farvid M, Feigin V, Ding EL, Fowkes G, Gebrehiwot T, Gillum R, Gold A, Gona P, Gupta R, Habtewold TD, Hafezi-Nejad N, Hailu T, Hailu GB, Hankey G, Hassen HY, Abate KH, Havmoeller R, Hay SI, Horino M, Hotez PJ, Jacobsen K, James S, Javanbakht M, Jeemon P, John D, Jonas J, Kalkonde Y, Karimkhani C, Kasaeian A, Khader Y, Khan A, Khang Y-H, Khera S, Khoja AT, Khubchandani J, Kim D, Kolte D, Kosen S, Krohn KJ, Kumar GA, Kwan GF, Lal DK, Larsson A, Linn S, Lopez A, et al. (2017) Global, Regional, and National Burden of Cardiovascular Diseases for 10 Causes, 1990 to 2015. *J Am Coll Cardiol* **70**:1–25.

Saito Y (2011) Pitavastatin: An overview. *Atheroscler Suppl* **12**:271–276.

Singhvi S, Pan H, Morrison R, and Willard D (1990) Disposition of pravastatin sodium, a tissue-selective HMG-CoA reductase inhibitor, in healthy subjects. *Br J Clin Pharmacol* **29**:239–243.

Slater EE, and MacDonald JS (1988) Mechanism of Action and Biological Profile of HMG CoA Reductase Inhibitors: A New Therapeutic Alternative. *Drugs* **36**:72–82.

Tse FLS, Jaffe JM, and Troendle A (1992) Pharmacokinetics of Fluvastatin After Single and Multiple Doses in Normal Volunteers. *J Clin Pharmacol* **32**:630–638.

van de Wetering K, Burkon A, Feddema W, Bot A, de Jonge H, Somoza V, and Borst P (2009) Intestinal Breast Cancer Resistance Protein (BCRP)/Bcrp1 and Multidrug Resistance Protein 3 (MRP3)/Mrp3 Are Involved in the Pharmacokinetics of Resveratrol. *Mol Pharmacol* **75**:876–885.

Vildhede A, Mateus A, Khan EK, Lai Y, Karlgren M, Artursson P, and Kjellsson MC (2016) Mechanistic Modeling of Pitavastatin Disposition in Sandwich-Cultured Human Hepatocytes: A Proteomics-Informed Bottom-Up Approach. *Drug Metab Dispos* **44**:505–516.

Yebyo HG, Aschmann HE, Kaufmann M, and Puhan MA (2019) Comparative effectiveness and safety of statins as a class and of specific statins for primary prevention of cardiovascular disease: A systematic review, meta-analysis, and network meta-analysis of randomized trials with 94,283 participants. *Am Heart J* **210**:18–28.

Zhou Q, Chen Q, Ruan Z-R, Yuan H, Xu H-M, and Zeng S (2013) CYP2C9*3(1075A > C), ABCB1 and SLCO1B1 genetic polymorphisms and gender are determinants of inter-subject variability in pitavastatin pharmacokinetics. *Pharm* **68**:187–194.

DMD Fast Forward. Published on June 23, 2021 as DOI: 10.1124/dmd.121.000430
This article has not been copyedited and formatted. The final version may differ from this version.

Footnotes

a. # This work was supported by the ERC Consolidator Grant (Grant Agreement number 725249).

b. The authors declare no conflict of interest.

c. This work has not been presented in any meeting. Parts of this work are included in the Master's Thesis of Suvi-Kukka Tuomi.

d. Reprint requests can be addressed to Prof. Mikko Niemi, P.O. Box 20, 00014 University of Helsinki, Finland, E-mail: mikko.niemi@helsinki.fi

e. [1] These authors contributed equally.

DMD Fast Forward. Published on June 23, 2021 as DOI: 10.1124/dmd.121.000430
This article has not been copyedited and formatted. The final version may differ from this version.

Legends for figures

Figure 1: The uptake of statins and atorvastatin metabolites in BCRP, MRP2, MRP3, MRP4, MRP8, P-gp and control vesicles. Statin concentrations, incubation time, and amount of vesicles were 10 µM (simvastatin acid 1 µM), 10 min, and 7.5 µg, respectively. Incubation time and the amount of vesicles in each experiment were 10 min and 7.5 µg, respectively. Black and grey bars represent statin uptake in vesicles in the presence and absence of ATP, respectively. Results are presented as mean ± SD transport obtained from a single experiment, performed with triplicate samples. One-way ANOVA was performed to evaluate whether the uptake ratio in transporter of interest differed from the control vesicles. * $p < 0.05$, ** $p < 0.01$

Figure 2: Concentration-dependent transport of atorvastatin in BCRP, MRP3, and P-gp vesicles. The time of incubation and vesicle amount were 5 min and 7.5 µg, respectively. Results are presented as mean ± SD transport, which is calculated from the means of each separate experiment. In total, three separate experiments were performed for each transporter with triplicate samples in each experiment.

Figure 3: Concentration-dependent transport of fluvastatin in BCRP, MRP2, MRP3, MRP4, MRP8, P-gp, and control vesicles. The time of incubation and vesicle amount were 5 min and 7.5 µg, respectively. Results are presented as mean ± SD transport, which is calculated from the means of each separate experiment. In total, three separate experiments were performed for each transporter with triplicate samples in each experiment.

Figure 4: Concentration-dependent transport of pitavastatin in BCRP, MRP3, P-gp, and control vesicles. The time of incubation and vesicle amount were 5 min and 7.5 µg, respectively. Results are presented as mean ± SD transport, which is calculated from the means of each separate experiment. In

DMD Fast Forward. Published on June 23, 2021 as DOI: 10.1124/dmd.121.000430
This article has not been copyedited and formatted. The final version may differ from this version.

total, three separate experiments (two for control vesicles) were performed for each transporter with triplicate samples in each experiment.

Figure 5: Concentration-dependent transport of pravastatin in MRP3 vesicles. The time of incubation and vesicle amount were 5 min and 7.5 µg, respectively. Results are presented as mean ± SD transport, which is calculated from the means of each separate experiment. In total, four separate experiments were performed with triplicate samples in each experiment.

Figure 6: Concentration-dependent transport of rosuvastatin in BCRP, MRP4, and P-gp vesicles. The time of incubation and vesicle amount were 5 min and 7.5 µg, respectively. Results are presented as mean ± SD transport, which is calculated from the means of each separate experiment. In total, three separate experiments were performed for MRP4 and P-gp with triplicate samples in each experiment. The BCRP results are from a single representative experiment with triplicate samples, where data is presented as mean ± SD transport.

Figure 7: The estimated total active tissue efflux clearance (expressed in nL/min/mg of tissue) and the individual contribution of ABC transporters to the total active tissue efflux clearance in duodenum, jejunum, ileum, and liver based on *in vitro* transport data and proteomic measurements. The contribution of efflux SLC transporters, drug metabolism and passive permeability on total clearance is not shown here.

DMD Fast Forward. Published on June 23, 2021 as DOI: 10.1124/dmd.121.000430
This article has not been copyedited and formatted. The final version may differ from this version.

Tables

Table 1: The summary of kinetic parameters and expression-adjusted clearance of atorvastatin, racemic fluvastatin, pitavastatin, pravastatin and rosuvastatin transport in BCRP, MRP2, MRP3, MRP4, MRP8, and P-gp vesicles. The 95% confidence intervals (95% CI) for the derived parameters are presented in parentheses.

Statin	Transporter	V_{max}, pmol/min/mg (95% CI)	K_m, µM (95% CI)	$CL_{in\ vitro}$, µL/min/mg	CL_{adj} nL/min/pmol of transporter
Atorvastatin	BCRP	135 (92.3 - 258)	82.4 (34.05 - 249)	1.6	30.8
	MRP3	77.0 (57.7 - 114)	31.5 (12.3 - 84.2)	2.4	68.7
	P-gp	32.9 (27.3 - 40.0)	10.7 (4.34 - 23.1)	3.1	133
Fluvastatin	BCRP	408 (313 - 580)	25.8 (9.81 - 68.4)	15.8	298
	MRP2	105 (45.2 - infinity)	54.0 (1.92 - infinity)	1.9	49.9
	MRP3	170 (77.1 - infinity)	48.9 (2.12 - infinity)	3.5	97.6
	MRP4	54.7 (23.4 - 4,053)	31.8 (0 - infinity)	1.7	76.4
	MRP8	74.5 (41.6 - 580)	73.0 (10.5 – 1,524)	1.0	n/a
	P-gp	169 (51.6 - infinity)	282 (21.3 - infinity)	0.6	25.8
Pitavastatin	BCRP	115 (98.1 - 137)	15.8 (6.53 - 32.4)	7.3	138
	MRP3	17.2 (10.7 - 29.0)	8.97 (0 - 73.3)	1.9	54.1
	P-gp	31.8 (18.3 - 97.4)	36.6 (3.64 - 316)	0.9	37.4
Pravastatin	MRP3	n/d	n/d	0.2	5.6
Rosuvastatin	BCRP	86.5 (71.4 - 106)	4.24 (2.02 - 8.44)	20.4	385
	MRP4	12.3 (5.13 - infinity)	39.3 (0.28 - infinity)	0.3	13.9
	P-gp	19.1 (11.3 - 51.8)	46.2 (5.7 - 344)	0.4	17.8

DMD Fast Forward. Published on June 23, 2021 as DOI: 10.1124/dmd.121.000430
This article has not been copyedited and formatted. The final version may differ from this version.

Figures

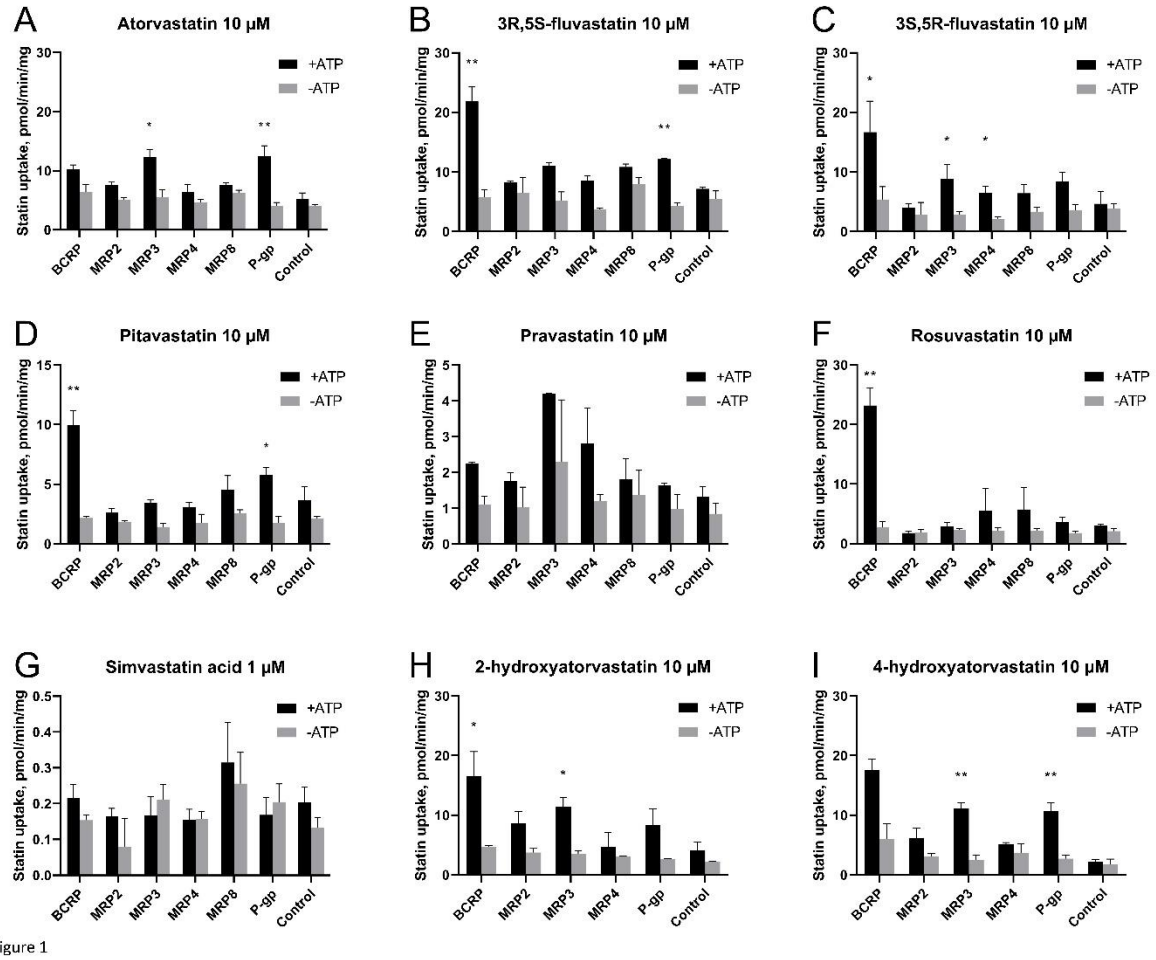

Figure 1

Figure 1: The uptake of statins and atorvastatin metabolites in BCRP, MRP2, MRP3, MRP4, MRP8, P-gp and control vesicles. Statin concentrations, incubation time, and amount of vesicles were 10 µM (simvastatin acid 1 µM), 10 min, and 7.5 µg, respectively. Incubation time and the amount of vesicles in each experiment were 10 min and 7.5 µg, respectively. Black and grey bars represent statin uptake in vesicles in the presence and absence of ATP, respectively. Results are presented as mean ± SD transport obtained from a single experiment, performed with triplicate samples. One-way ANOVA was performed to evaluate whether the uptake ratio in transporter of interest differed from the control vesicles. * $p < 0.05$, ** $p < 0.01$

DMD Fast Forward. Published on June 23, 2021 as DOI: 10.1124/dmd.121.000430
This article has not been copyedited and formatted. The final version may differ from this version.

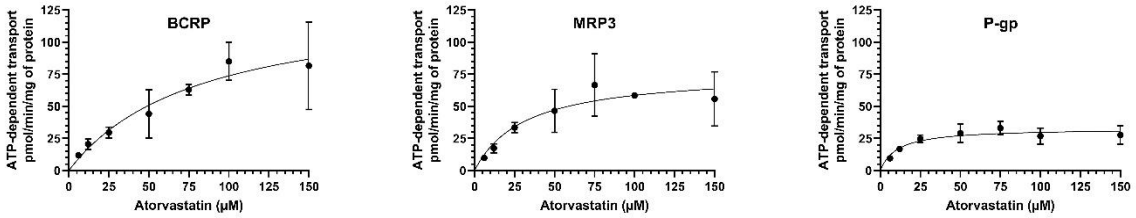

Figure 2

Figure 2: Concentration-dependent transport of atorvastatin in BCRP, MRP3, and P-gp vesicles. The time of incubation and vesicle amount were 5 min and 7.5 µg, respectively. Results are presented as mean ± SD transport, which is calculated from the means of each separate experiment. In total, three separate experiments were performed for each transporter with triplicate samples in each experiment.

DMD Fast Forward. Published on June 23, 2021 as DOI: 10.1124/dmd.121.000430
This article has not been copyedited and formatted. The final version may differ from this version.

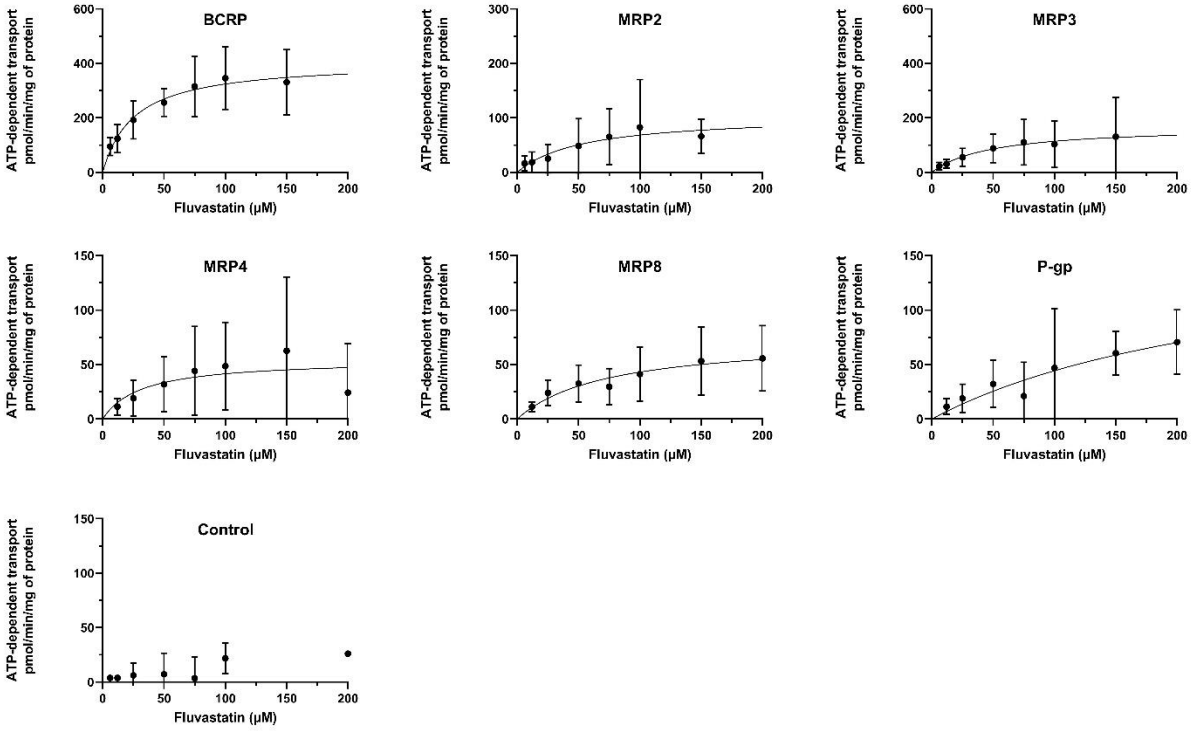

Figure3

Figure 3: Concentration-dependent transport of fluvastatin in BCRP, MRP2, MRP3, MRP4, MRP8, P-gp, and control vesicles. The time of incubation and vesicle amount were 5 min and 7.5 µg, respectively. Results are presented as mean ± SD transport, which is calculated from the means of each separate experiment. In total, three separate experiments were performed for each transporter with triplicate samples in each experiment.

DMD Fast Forward. Published on June 23, 2021 as DOI: 10.1124/dmd.121.000430
This article has not been copyedited and formatted. The final version may differ from this version.

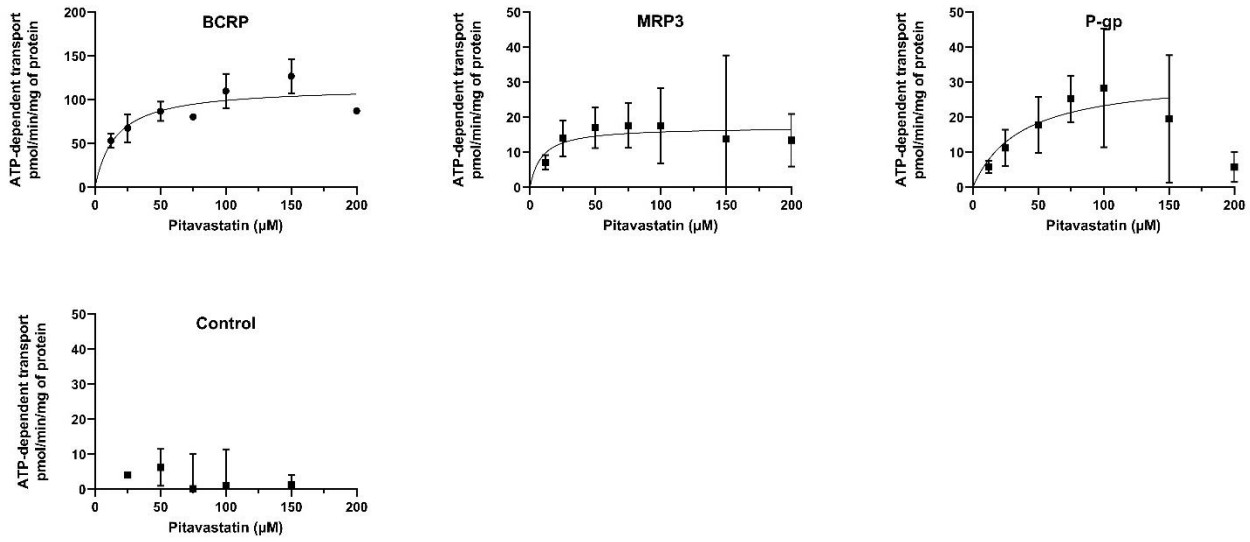

Figure 4

Figure 4: Concentration-dependent transport of pitavastatin in BCRP, MRP3, P-gp, and control vesicles. The time of incubation and vesicle amount were 5 min and 7.5 μg, respectively. Results are presented as mean ± SD transport, which is calculated from the means of each separate experiment. In total, three separate experiments (two for control vesicles) were performed for each transporter with triplicate samples in each experiment.

DMD Fast Forward. Published on June 23, 2021 as DOI: 10.1124/dmd.121.000430
This article has not been copyedited and formatted. The final version may differ from this version.

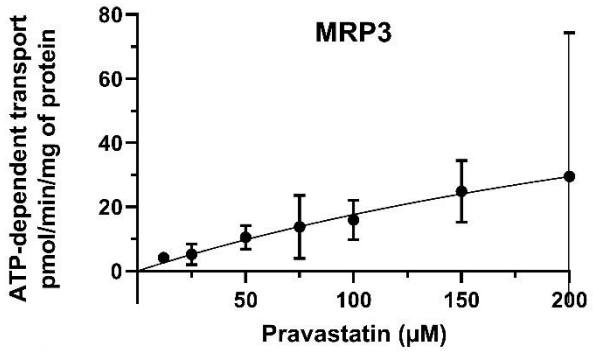

Figure 5

Figure 5: Concentration-dependent transport of pravastatin in MRP3 vesicles. The time of incubation and vesicle amount were 5 min and 7.5 μg, respectively. Results are presented as mean ± SD transport, which is calculated from the means of each separate experiment. In total, four separate experiments were performed with triplicate samples in each experiment.

DMD Fast Forward. Published on June 23, 2021 as DOI: 10.1124/dmd.121.000430
This article has not been copyedited and formatted. The final version may differ from this version.

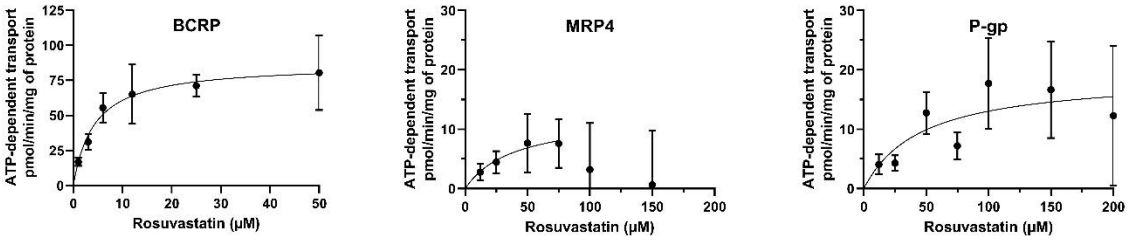

Figure 6

Figure 6: Concentration-dependent transport of rosuvastatin in BCRP, MRP4, and P-gp vesicles. The time of incubation and vesicle amount were 5 min and 7.5 µg, respectively. Results are presented as mean ± SD transport, which is calculated from the means of each separate experiment. In total, three separate experiments were performed for MRP4 and P-gp with triplicate samples in each experiment. The BCRP results are from a single representative experiment with triplicate samples, where data is presented as mean ± SD transport.

DMD Fast Forward. Published on June 23, 2021 as DOI: 10.1124/dmd.121.000430
This article has not been copyedited and formatted. The final version may differ from this version.

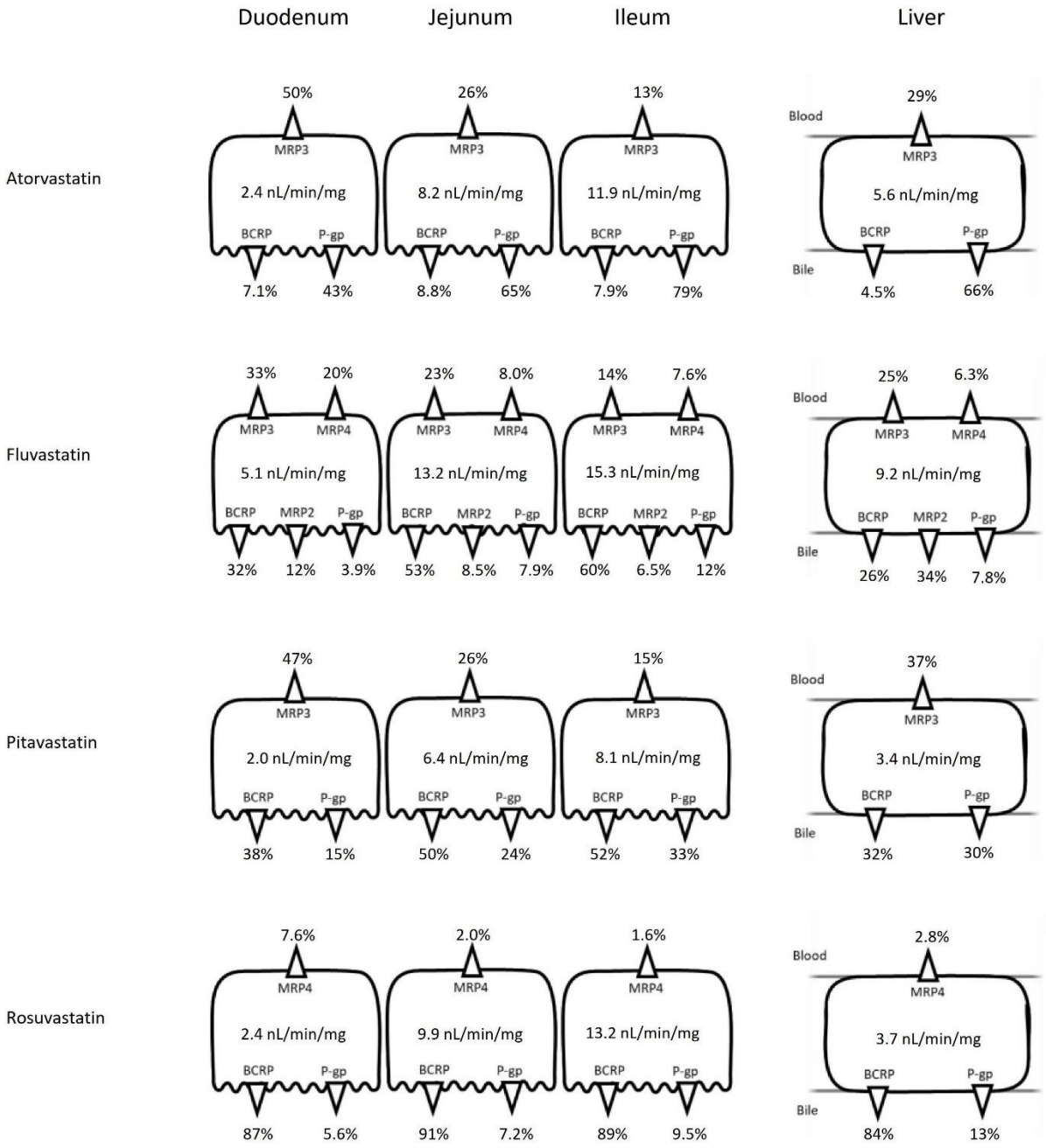

Figure 7

Figure 7: The estimated total active tissue efflux clearance (expressed in nL/min/mg of tissue) and the individual contribution of ABC transporters to the total active tissue efflux clearance in duodenum, jejunum, ileum, and liver based on *in vitro* transport data and proteomic measurements. The contribution of efflux SLC transporters, drug metabolism and passive permeability on total clearance is not shown here.

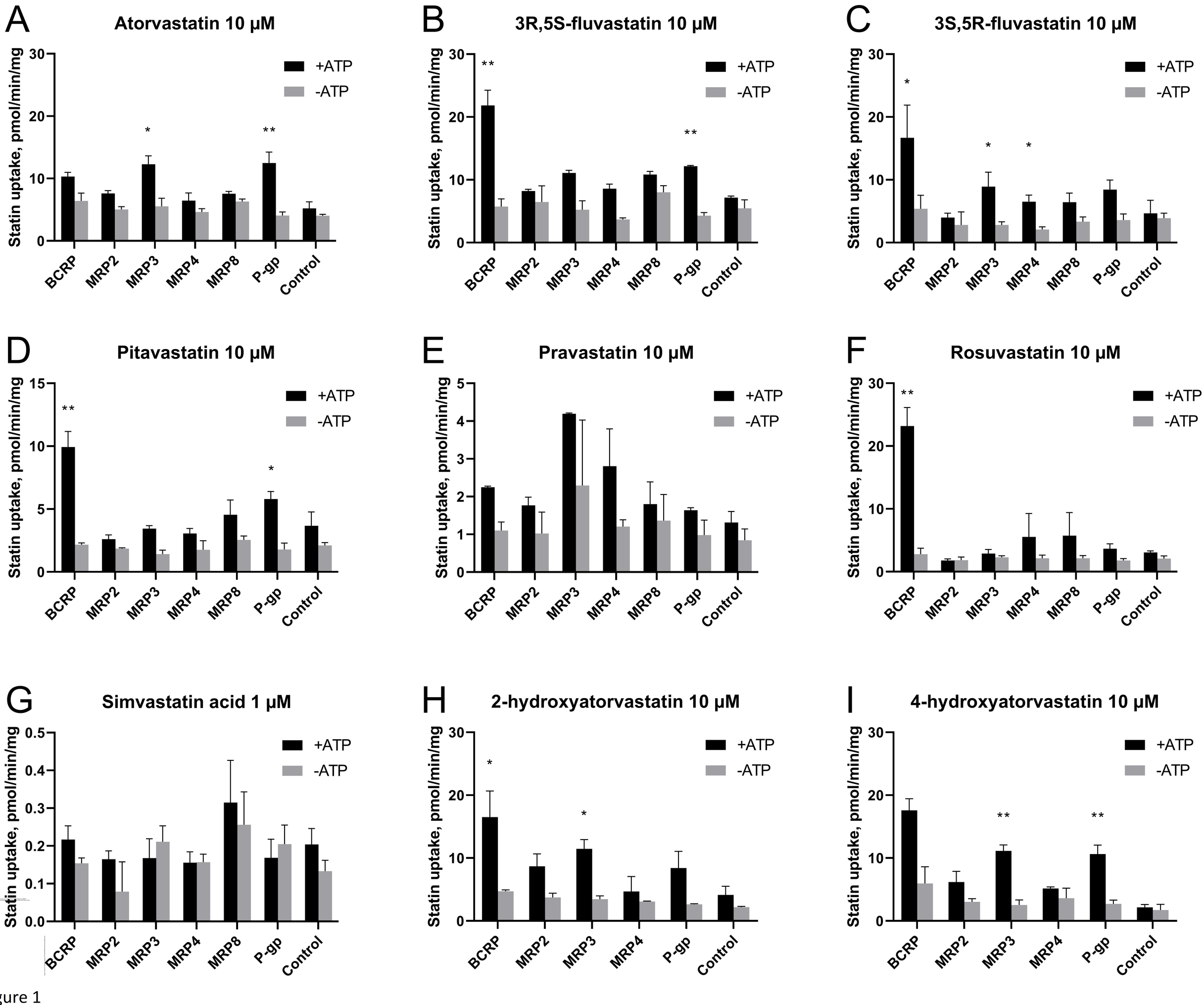
A
Atorvastatin 10 µM
B
3R,5S-fluvastatin 10 µM
C
3S,5R-fluvastatin 10 µM
D
Pitavastatin 10 µM
E
Pravastatin 10 µM
F
Rosuvastatin 10 µM
G
Simvastatin acid 1 µM
H
2-hydroxyatorvastatin 10 µM
I
4-hydroxyatorvastatin 10 µM
Statin uptake, pmol/min/mg
+ATP
-ATP
BCRP
MRP2
MRP3
MRP4
MRP8
P-gp
Control

Figure 1

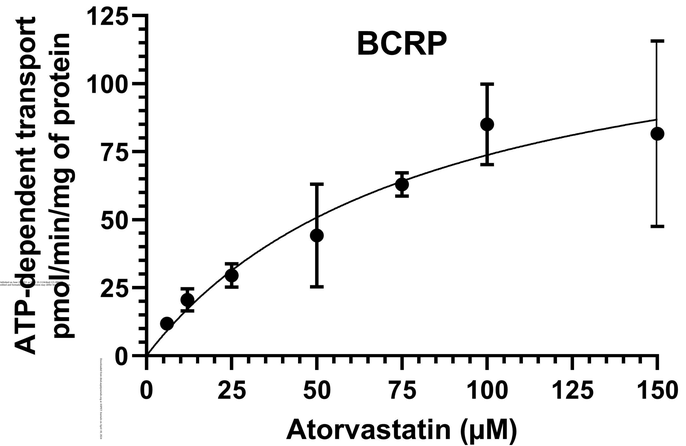
BCRP
ATP-dependent transport
pmol/min/mg of protein
125
100
75
50
25
0
0
25
50
75
100
125
150
Atorvastatin (μM)

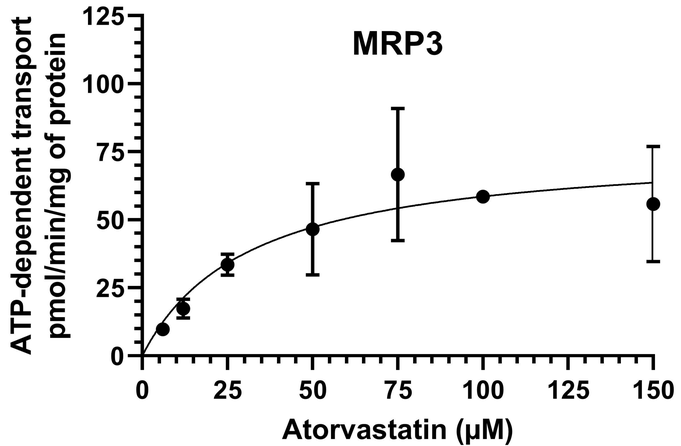
MRP3
ATP-dependent transport
pmol/min/mg of protein
125
100
75
50
25
0
0
25
50
75
100
125
150
Atorvastatin (μM)

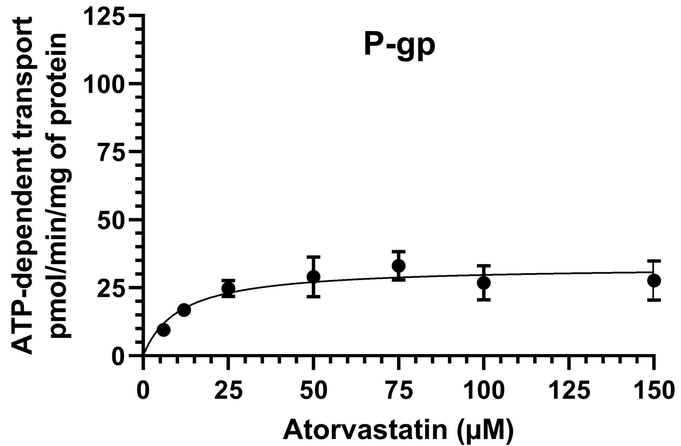
P-gp
ATP-dependent transport
pmol/min/mg of protein
125
100
75
50
25
0
0
25
50
75
100
125
150
Atorvastatin (μM)

Figure 2

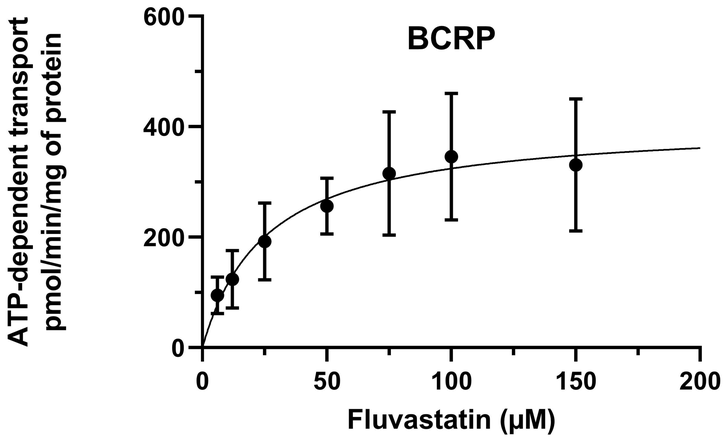
BCRP
ATP-dependent transport
pmol/min/mg of protein
0
200
400
600
0
50
100
150
200
Fluvastatin (μM)

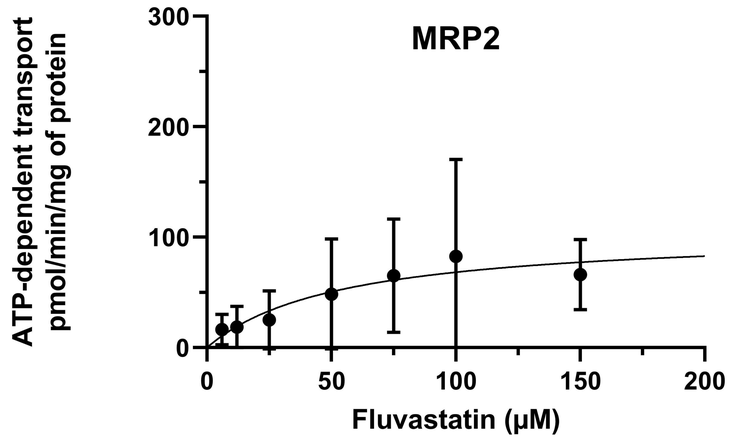
MRP2
ATP-dependent transport
pmol/min/mg of protein
0
100
200
300
0
50
100
150
200
Fluvastatin (μM)

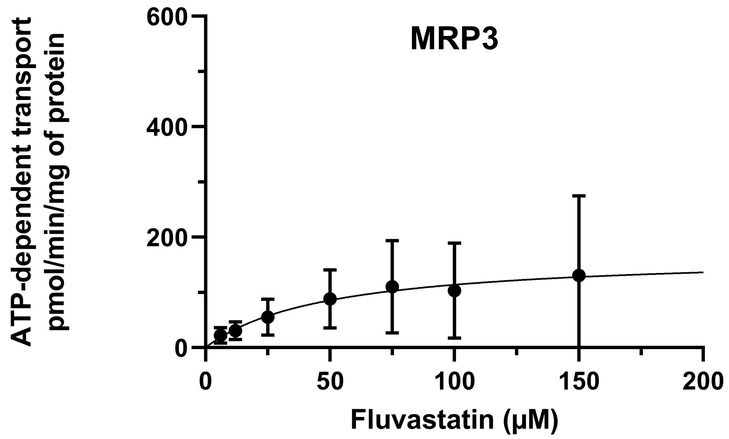
MRP3
ATP-dependent transport
pmol/min/mg of protein
0
200
400
600
0
50
100
150
200
Fluvastatin (μM)

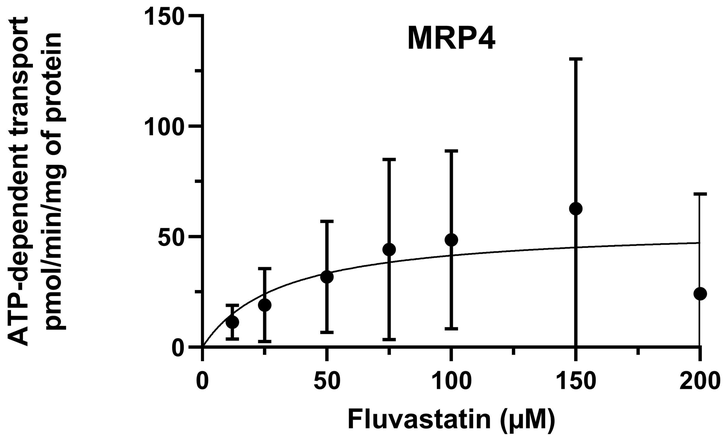
MRP4
ATP-dependent transport
pmol/min/mg of protein
0
50
100
150
0
50
100
150
200
Fluvastatin (μM)

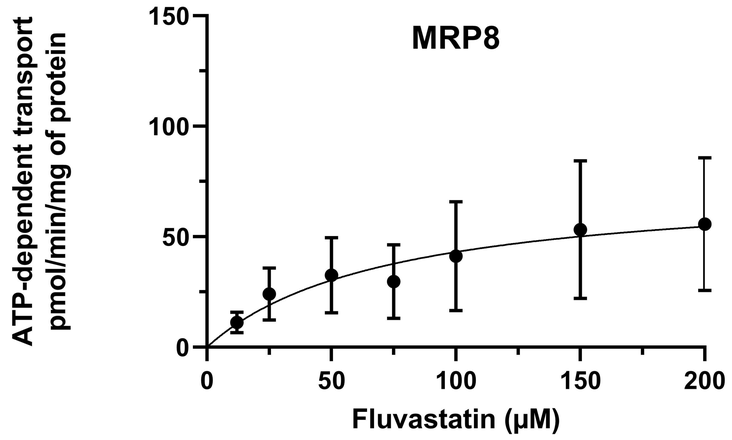
MRP8
ATP-dependent transport
pmol/min/mg of protein
0
50
100
150
0
50
100
150
200
Fluvastatin (μM)

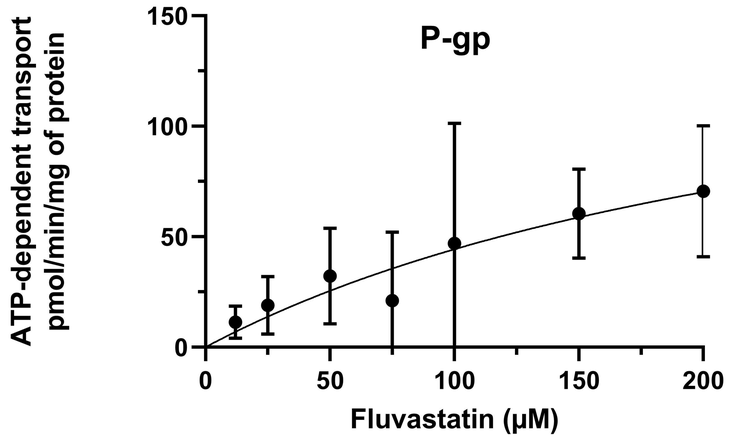
P-gp
ATP-dependent transport
pmol/min/mg of protein
0
50
100
150
0
50
100
150
200
Fluvastatin (μM)

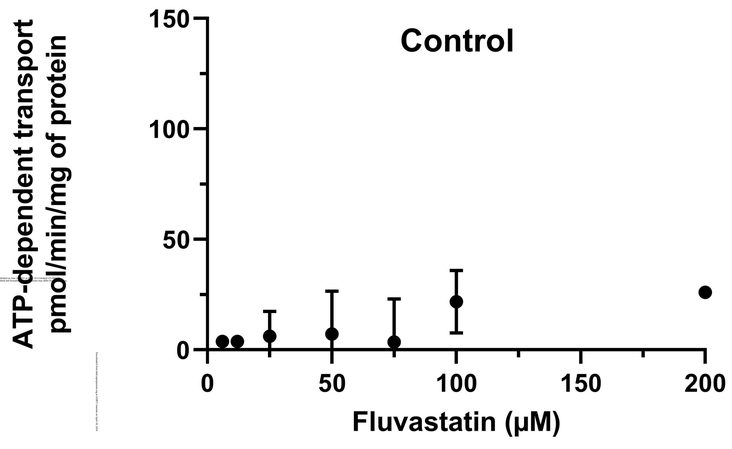
Control
ATP-dependent transport
pmol/min/mg of protein
0
50
100
150
0
50
100
150
200
Fluvastatin (μM)

Figure3

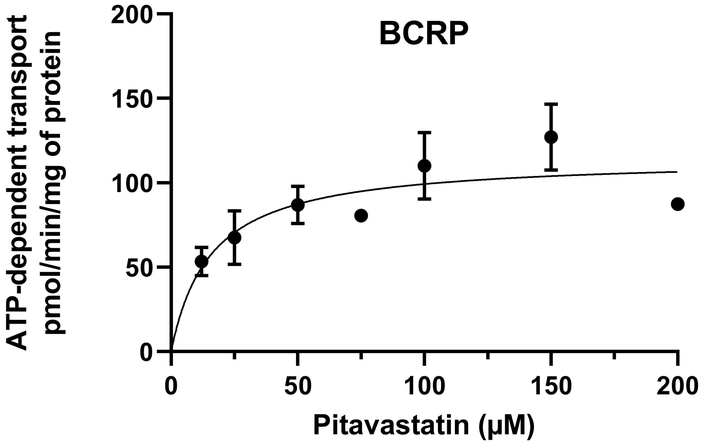
BCRP
ATP-dependent transport
pmol/min/mg of protein
0
50
100
150
200
Pitavastatin (μM)

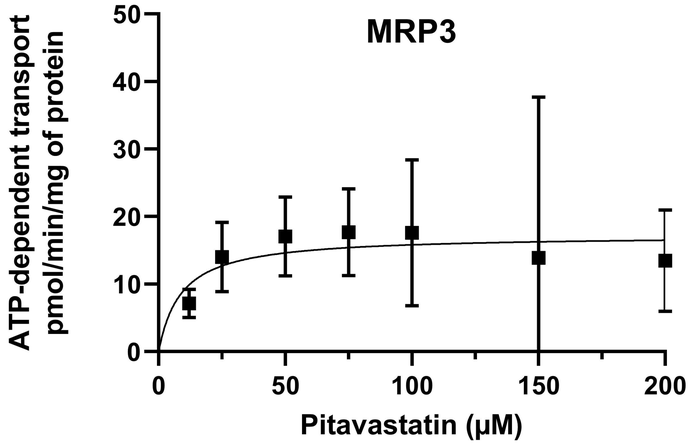
MRP3
ATP-dependent transport
pmol/min/mg of protein
0
10
20
30
40
50
0
50
100
150
200
Pitavastatin (μM)

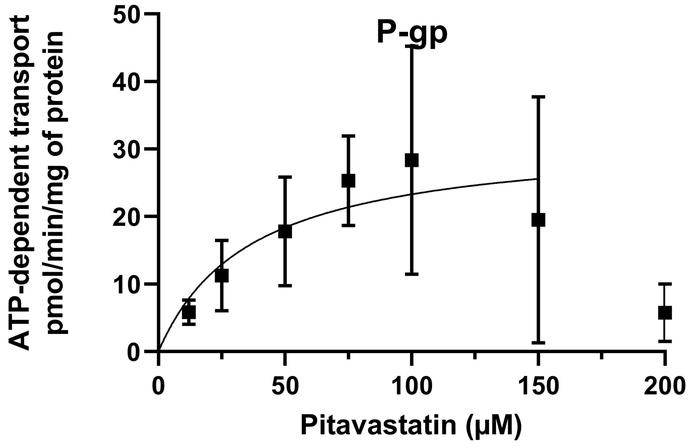
P-gp
ATP-dependent transport
pmol/min/mg of protein
0
10
20
30
40
50
0
50
100
150
200
Pitavastatin (μM)

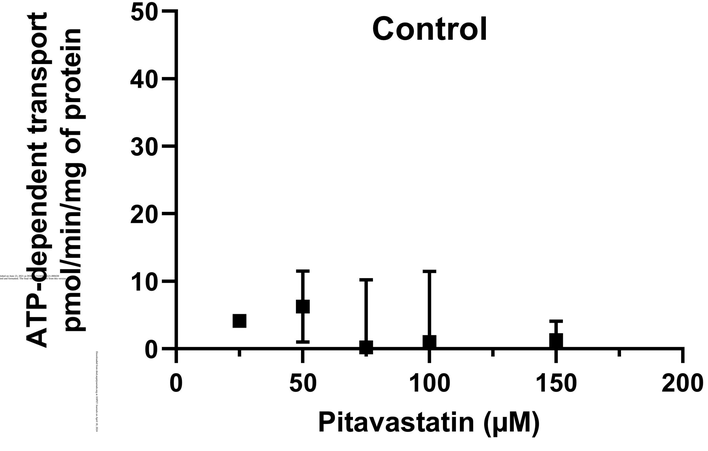
Control
ATP-dependent transport
pmol/min/mg of protein
0
10
20
30
40
50
0
50
100
150
200
Pitavastatin (μM)

Figure 4

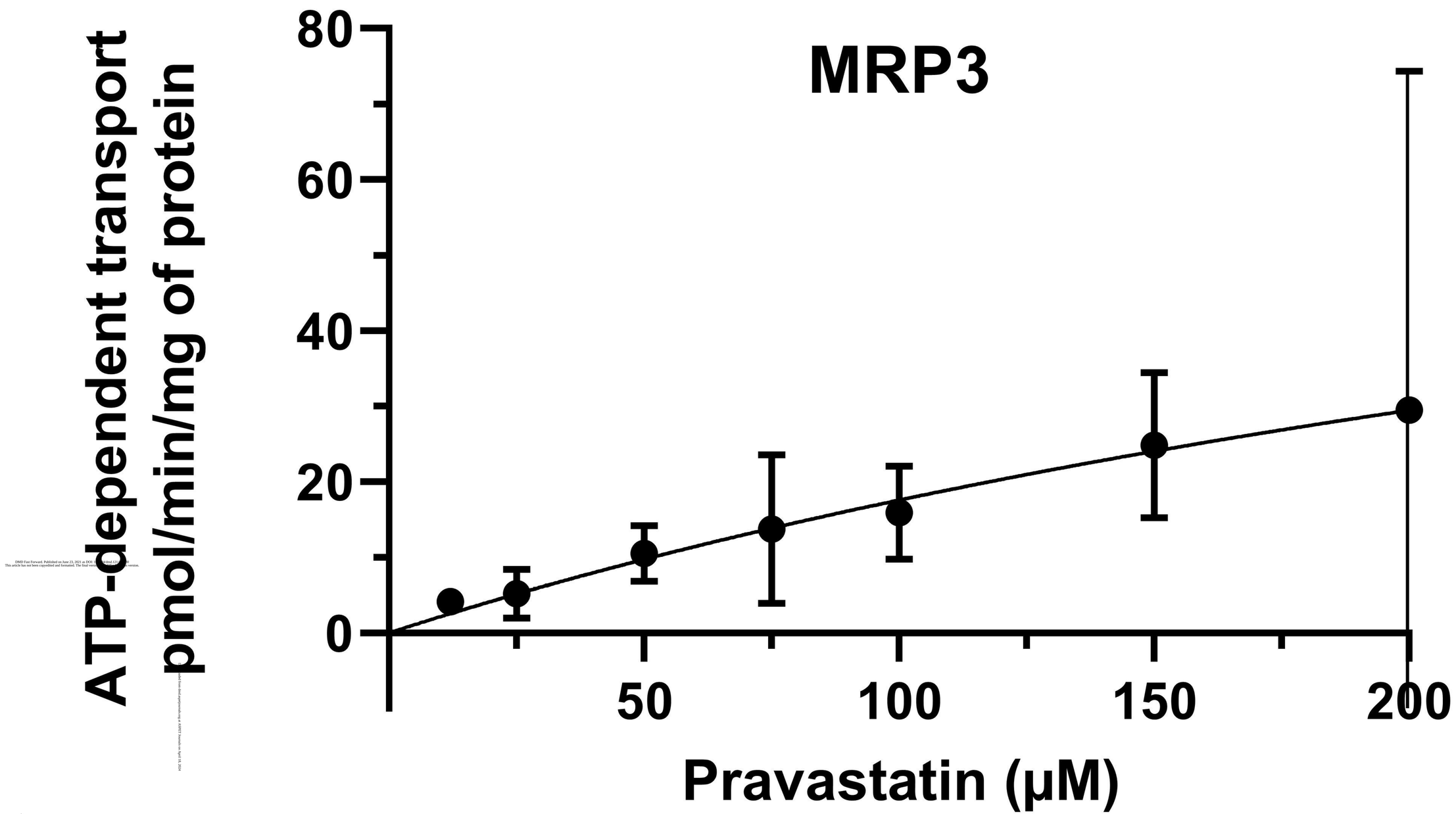

Figure 5

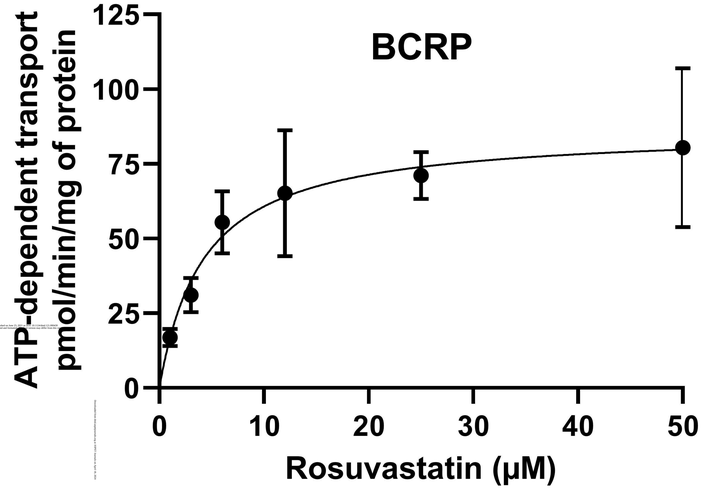
BCRP
ATP-dependent transport
pmol/min/mg of protein
125
100
75
50
25
0
0
10
20
30
40
50
Rosuvastatin (μM)

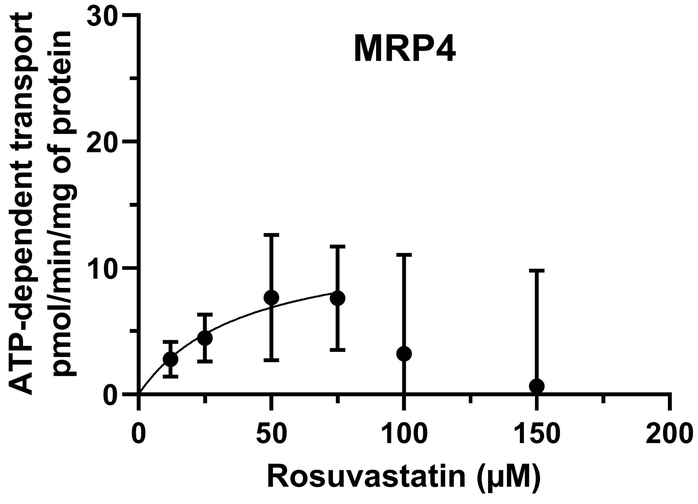
MRP4
ATP-dependent transport
pmol/min/mg of protein
30
20
10
0
0
50
100
150
200
Rosuvastatin (μM)

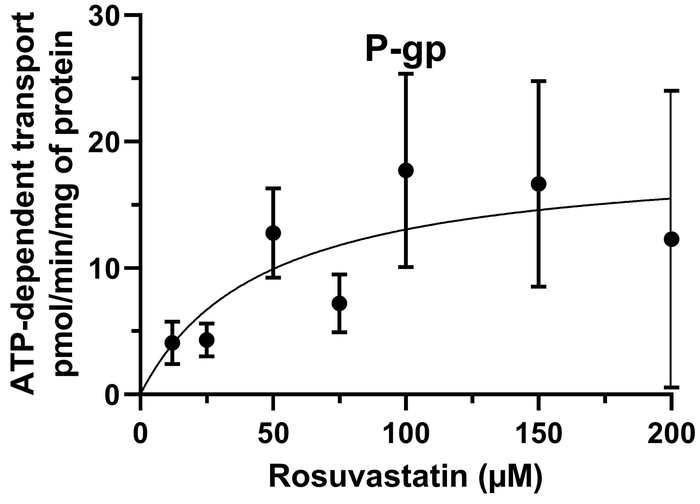
P-gp
ATP-dependent transport
pmol/min/mg of protein
30
20
10
0
0
50
100
150
200
Rosuvastatin (μM)

Figure 6

DMD Fast Forward. Published on June 23, 2021 as DOI: 10.1124/dmd.121.000430
This article has not been copyedited and formatted. The final version may differ from this version.

Figure 7

Supporting information

Comparative hepatic and intestinal efflux transport of statins

Feng Deng, Suvi-Kukka Tuomi, Mikko Neuvonen, Päivi Hirvensalo, Sami Kulju, Christoph Wenzel, Stefan Oswald, Anne M. Filppula, Mikko Niemi

Department of Clinical Pharmacology, Faculty of Medicine, University of Helsinki, Helsinki, Finland (F.D., S.K.T., M.Ne., P.H., S.K., A.M.F., M.Ni.)

Individualized Drug Therapy Research Program, Faculty of Medicine, University of Helsinki, Helsinki, Finland (F.D., S.K.T., M.Ne., P.H., S.K., A.M.F., M.Ni.)

Institute of Pharmacology, Center of Drug Absorption and Transport, University Medicine Greifswald, Greifswald, Germany (C.W., S.O.)

Institute of Pharmacology and Toxicology, Rostock University Medical Center, Rostock, Germany (S.O.)

Department of Clinical Pharmacology, HUS Diagnostic Center, Helsinki University Hospital, Helsinki, Finland (M.Niemi)

Corresponding author: Mikko Niemi, Department of Clinical Pharmacology, Faculty of Medicine

Supplementary table S1: The characteristic multiple reaction monitoring (MRM) transitions of the analytes and internal standards.

Analyte	Analyte mass-to-charge ratios (m/z)	Internal standard (concentration in stop solution)	Internal standard mass-to-charge ratios (m/z)	Ionization (+/-)	Limit of quantification (analyte)
Atorvastatin	559.1-440.1	Atorvastatin-d5 (25 ng/ml)	564.1-445.1	Positive	0.077 nM
2-hydroxyatorvastatin	575.1-440.1	2-hydroxyatorvastatin-d5 (25 ng/ml)	580.1-445.1	Positive	0.185 nM
2-hydroxyatorvastatin lactone	557.1-448.1	2-hydroxyatorvastatin lactone-d5 (25 ng/ml)	562.1-453.1	Positive	0.741 nM
4-hydroxyatorvastatin	575.1-440.1	4-hydroxyatorvastatin-d5 (25 ng/ml)	580.1-445.1	Positive	0.167 nM
4-hydroxyatorvastatin lactone	557.1-448.1	4-hydroxyatorvastatin lactone-d5 (25 ng/ml)	562.1-453.1	Positive	0.741 nM
Fluvastatin (racemic)	410.1-348.1	Fluvastatin-d8 (25 ng/ml)	418.1-356.1	Negative	0.226 nM
3R,5S-fluvastatin	410.1-348.1	Fluvastatin-d8 (25 ng/ml)	418.1-356.1	Negative	0.226 nM
3S,5R-fluvastatin	410.1-348.1	Fluvastatin-d8 (25 ng/ml)	418.1-356.1	Negative	0.226 nM
Pitavastatin	422.1-290.1	Pitavastatin-d5 (25 ng/ml)	427.1-295.1	Positive	0.3 nM
Pravastatin	442.1-269.1	Pravastatin-d9 (25 ng/ml)	451.1-269.1	Positive	0.29 nM
Rosuvastatin	482.1-258.1	Rosuvastatin-d6 (25 ng/ml)	488.1-264.1	Positive	0.29 nM
Simvastatin acid	437.1-303.1	Simvastatin acid-d6 (25 ng/ml)	443.1-303.1	Positive	0.293 nM
Estradiol-17-glucuronide	471-199	Tauroursodeoxycholic acid -d5 (20 ng/ml)	503-80	Positive/ Negative	N.D.
N-methyl-quinidine	339-58	Quinine-d3 (25 ng/ml)	328-79	Positive	N.D.

Supplementary table S2: Summary of screening results. The mean and SD of uptake in the presence (+ATP) and absence of ATP (-ATP), ATP-dependent transport, and ratio of statin uptake between +ATP and –ATP from each transport-statin combination were obtained from a single experiment, performed with triplicate samples. One-way ANOVA was performed to evaluate the transport rates and the uptake ratio compared to control. * $p < 0.05$, ** $p < 0.01$.

Statin	Transporter	+ATP (pmol/min/mg)	SD	-ATP (pmol/min/mg)	SD	ATP-dependent transport (pmol/min/mg)	SD		Uptake ratio of +ATP / -ATP	SD	
10 µM atorvastatin	BCRP	10.32	0.66	6.42	1.24	3.90	1.41	*	1.61	0.33	
	MRP2	7.61	0.45	5.04	0.46	2.57	0.64		1.51	0.16	
	MRP3	12.28	1.35	5.53	1.30	6.75	1.87	**	2.22	0.58	*
	MRP4	6.45	1.23	4.64	0.53	1.81	1.34		1.39	0.31	
	MRP8	7.56	0.39	6.30	0.41	1.26	0.57		1.20	0.10	
	P-gp	12.48	1.75	4.07	0.57	8.41	1.84	**	3.06	0.60	**
	Control	5.22	1.04	4.03	0.24	1.19	1.07		1.30	0.27	
10 µM 3R,5S-fluvastatin	BCRP	21.84	2.41	5.75	1.21	16.09	2.70	**	3.80	0.91	**
	MRP2	8.21	0.27	6.46	2.58	1.75	2.59		1.27	0.51	
	MRP3	11.08	0.44	5.24	1.43	5.84	1.49	*	2.12	0.58	
	MRP4	8.58	0.75	3.68	0.25	4.90	0.79		2.33	0.26	
	MRP8	10.83	0.50	8.01	1.05	2.82	1.16		1.35	0.19	
	P-gp	12.16	0.13	4.28	0.50	7.89	0.52	**	2.84	0.34	**
	Control	7.16	0.26	5.47	1.34	1.70	1.36		1.31	0.32	
10 µM 3S,5R-fluvastatin	BCRP	16.68	5.21	5.40	2.13	11.28	5.63	**	3.09	1.56	*
	MRP2	3.99	0.69	2.81	2.08	1.18	2.19		1.42	1.08	
	MRP3	8.91	2.31	2.81	0.51	6.10	2.37	*	3.17	1.00	*
	MRP4	6.51	1.05	2.08	0.43	4.43	1.14		3.13	0.82	*
	MRP8	6.43	1.44	3.34	0.75	3.09	1.63		1.92	0.61	
	P-gp	8.45	1.52	3.58	0.99	4.87	1.82		2.36	0.78	
	Control	4.67	2.06	3.89	0.80	0.78	2.21		1.20	0.58	
10 µM pitavastatin	BCRP	9.93	1.24	2.17	0.14	7.76	1.25	**	4.57	0.64	**
	MRP2	2.61	0.34	1.86	0.06	0.75	0.35		1.40	0.19	
	MRP3	3.44	0.24	1.42	0.31	2.02	0.40		2.43	0.56	
	MRP4	3.06	0.39	1.76	0.72	1.30	0.82		1.74	0.75	
	MRP8	4.54	1.17	2.54	0.31	2.00	1.21		1.79	0.51	
	P-gp	5.79	0.61	1.78	0.52	4.01	0.80	*	3.25	1.01	*
	Control	3.67	1.10	2.11	0.22	1.56	1.12		1.74	0.55	
10 µM pravastatin	BCRP	2.25	0.03	1.10	0.22	1.15	0.23		2.04	0.42	
	MRP2	1.77	0.22	1.02	0.57	0.75	0.61		1.73	0.99	
	MRP3	4.19	0.02	2.29	1.73	1.90	1.73		1.83	1.38	
	MRP4	2.81	0.98	1.21	0.18	1.60	1.00		2.33	0.89	
	MRP8	1.80	0.59	1.36	0.69	0.44	0.91		1.32	0.80	
	P-gp	1.64	0.07	0.98	0.39	0.66	0.40		1.67	0.68	
	Control	1.31	0.29	0.84	0.30	0.47	0.42		1.55	0.65	
10 µM rosuvastatin	BCRP	23.19	2.93	2.78	0.95	20.42	3.08	**	8.35	3.05	**
	MRP2	1.80	0.23	1.84	0.49	-0.05	0.55		0.97	0.29	
	MRP3	2.88	0.66	2.29	0.24	0.59	0.71		1.26	0.32	
	MRP4	5.53	3.72	2.14	0.49	3.39	3.75		2.59	1.84	
	MRP8	5.73	3.68	2.15	0.42	3.59	3.71		2.67	1.79	
	P-gp	3.65	0.78	1.79	0.29	1.87	0.83		2.04	0.55	
	Control	3.07	0.24	2.09	0.41	0.98	0.48		1.47	0.31	
1 µM simvastatin	BCRP	0.22	0.04	0.15	0.01	0.06	0.04		1.40	0.27	
	MRP2	0.16	0.02	0.08	0.08	0.09	0.08		2.08	2.09	
	MRP3	0.17	0.05	0.21	0.04	-0.04	0.07		0.79	0.29	
	MRP4	0.16	0.03	0.16	0.02	0.00	0.04		0.99	0.22	
	MRP8	0.31	0.11	0.26	0.09	0.06	0.14		1.23	0.60	
	P-gp	0.17	0.05	0.20	0.05	-0.04	0.07		0.82	0.31	
	Control	0.20	0.04	0.13	0.03	0.07	0.05		1.53	0.46	

Supplementary table S3: Summary of atorvastatin metabolite transport. The mean and SD of uptake in the presence (+ATP) and absence of ATP (-ATP), ATP-dependent transport and ratio between +ATP and –ATP from each transport-metabolite combination were obtained from a single experiment, performed with triplicate samples. One-way ANOVA was performed to evaluate the transport rates and the uptake ratio compared to control. * $p < 0.05$, ** $p < 0.01$

Metabolite	Transporter	+ATP (pmol/min/mg)	SD	-ATP (pmol/min/mg)	SD	ATP-dependent transport (pmol/min/mg)	SD		Uptake ratio of +ATP / -ATP	SD	
10 µM 2OH-ATV	BCRP	16.52	4.14	4.72	0.22	11.80	4.15	**	3.50	0.89	*
	MRP2	8.68	1.98	3.74	0.67	4.94	2.09		2.32	0.67	
	MRP3	11.47	1.47	3.47	0.51	8.00	1.55	*	3.30	0.64	*
	MRP4	4.69	2.36	3.08	0.08	1.61	2.36		1.52	0.77	
	P-gp	8.42	2.64	2.63	0.11	5.79	2.65		3.20	1.01	
	Control	4.13	1.39	2.18	0.14	1.95	1.39		1.90	0.65	
10 µM 4OH-ATV	BCRP	17.58	1.87	5.96	2.65	11.61	3.24	**	2.95	1.34	
	MRP2	6.18	1.71	3.05	0.50	3.13	1.78		2.02	0.65	
	MRP3	11.13	0.96	2.53	0.82	8.61	1.26	**	4.41	1.48	**
	MRP4	5.15	0.27	3.62	1.59	1.54	1.61		1.42	0.63	
	P-gp	10.64	1.41	2.70	0.62	7.95	1.54	**	3.95	1.05	**
	Control	2.16	0.45	1.73	0.92	0.44	1.02		1.25	0.71	
10 µM 2OH-ATV lac	BCRP	6.99	1.60	8.76	0.80	-1.77	1.79		0.80	0.20	
	MRP2	9.93	2.18	10.93	0.81	-1.00	2.32		0.91	0.21	
	MRP3	9.38	2.21	10.78	0.19	-1.40	2.21		0.87	0.21	
	MRP4	7.62	0.60	10.51	2.25	-2.89	2.33		0.73	0.17	
	P-gp	8.96	2.67	9.62	1.13	-0.66	2.90		0.93	0.30	
	Control	5.53	1.73	6.57	1.29	-1.04	2.16		0.84	0.31	
10 µM 4OH-ATV lac	BCRP	3.94	0.56	5.19	0.91	-1.24	1.07		0.76	0.17	
	MRP2	5.58	1.77	5.02	0.42	0.56	1.82		1.11	0.36	
	MRP3	4.90	0.65	6.03	1.69	-1.13	1.81		0.81	0.25	
	MRP4	4.48	0.57	5.20	0.97	-0.72	1.13		0.86	0.20	
	P-gp	4.38	0.63	4.96	0.42	-0.58	0.76		0.88	0.15	
	Control	4.03	0.57	4.29	0.88	-0.26	1.05		0.94	0.23	

Supplementary table S4: Summary of screening results. The mean and SD of uptake in the presence (+ATP) and absence of ATP (-ATP), ATP-dependent transport and ratio between +ATP and –ATP from each transport-statin combination studied were obtained from a single experiment, performed with triplicate samples. Two-way ANOVA was performed to evaluate the transport rate and uptake ratio compared to control. * $p < 0.05$, ** $p < 0.01$

Statin	Transporter	ATP-dependent transport at 5 min (pmol/min/mg)	SD		Ratio of +ATP / -ATP at 5min	SD		ATP-dep. transport at 10 min	SD		Ratio at 10 min	SD		ATP-dep. transport at 15 min	SD		Ratio at 15 min	SD	
Atorvastatin	BCRP	196.6	54.5	**	2.53	0.43	**	121.1	31.7	**	2.70	0.58	*	154.3	38.4	*	2.31	0.57	
	MRP2	66.7	19.1		1.61	0.21		90.7	13.3	*	2.09	0.27		69.3	25.4		1.75	0.41	
	MRP3	143.2	15.7	*	2.16	0.23	*	131.8	16.1	**	2.57	0.21	*	160.6	74.2	**	2.22	0.74	
	MRP4	43.8	5.8		1.49	0.09		53.4	3.8		1.75	0.08		54.2	9.8		1.71	0.15	
	P-gp	186.7	34.0	**	2.46	0.36	**	108.7	52.0	**	3.12	1.03	**	243.9	40.0	**	3.41	0.66	**
	Control	65.5	59.5		1.45	0.41		27.0	12.2		1.27	0.13		47.8	5.0		1.42	0.05	
3R,5S-fluvastatin	BCRP	344.9	92.8	**	4.05	0.85	**	408.3	39.9	**	4.10	0.55	**	416.6	56.7	**	4.05	0.84	**
	MRP2	84.8	9.5	*	2.33	0.17	**	118.9	10.8	**	2.60	0.25	**	100.6	12.7		2.52	0.29	
	MRP3	177.6	39.7	**	3.06	0.63	**	320.3	52.4	**	3.81	0.65	**	206.4	34.9	**	3.72	0.46	**
	MRP4	91.2	22.1	*	2.50	0.47	**	195.2	27.3	**	2.76	0.30	**	37.9	11.6		2.23	0.68	
	MRP8	136.7	11.3	**	2.03	0.12	*	10.8	8.6		1.36	0.30		41.6	12.1		1.73	0.26	
	P-gp	195.1	23.7	**	2.96	0.32	**	204.3	10.5	**	2.78	0.12	**	205.7	35.4	**	3.54	0.89	**
	Control	4.3	4.8		1.14	0.17		-1.8	5.4		0.97	0.10		54.1	19.3		1.83	0.44	
3S,5R-fluvastatin	BCRP	326.3	29.1	**	5.38	2.05	**	409.6	41.5	**	4.49	0.48	**	344.4	51.6	**	4.25	0.65	**
	MRP2	0.1	13.2		1.00	0.25		79.8	10.2	**	2.79	0.31	**	70.8	4.1		2.50	0.12	
	MRP3	128.5	25.6	**	3.07	0.75	*	157.3	26.8	**	3.47	0.50	**	179.8	14.5	**	4.19	0.43	**
	MRP4	49.6	9.5		2.16	0.45		99.1	13.1	**	3.56	0.82	**	91.5	16.8		2.91	0.74	
	MRP8	48.3	14.6		1.71	0.25		86.0	10.4	**	2.04	0.13		96.9	19.9		1.93	0.27	
	P-gp	124.9	18.6	**	2.74	0.33		182.2	12.8	**	3.08	0.32	**	182.9	55.4	**	2.52	0.72	
	Control	22.4	19.6		1.27	0.27		11.1	6.4		1.42	0.33		69.5	15.9		1.98	0.44	

Supplementary table S5: Summary of screening results. The mean and SD of uptake in the presence (+ATP) and absence of ATP (-ATP), ATP-dependent transport and ratio between +ATP and –ATP from each transport-statin combination studied were obtained from a single experiment, performed with triplicate samples. Two-way ANOVA was performed to evaluate the transport rate and uptake ratio compared to control. * $p < 0.05$, ** $p < 0.01$

Statin	Transporter	ATP-dependent transport at 5 min (pmol/min/mg)	SD		Ratio of +ATP / -ATP at 5min	SD		ATP-dep. transport at 10 min	SD		Ratio at 10 min	SD		ATP-dep. transport at 15 min	SD		Ratio at 15 min	SD	
Pitavastatin	BCRP	357.6	18.0	**	5.24	0.58	**	348.8	58.5	**	5.71	0.80	**	281.4	18.2	**	5.16	0.34	**
	MRP3	68.2	26.8	*	1.92	0.46		78.9	40.5		1.91	0.50		80.3	1.6	**	2.27	0.03	**
	MRP8	16.7	27.0		1.16	0.28		51.8	14.9		1.68	0.23		15.7	58.2		1.15	0.64	
	P-gp	100.1	15.4	**	3.63	1.12	**	74.2	7.5		2.82	0.46		12.8	7.3		1.64	0.53	
	Control – A	31.6	7.6		1.72	0.20		38.1	12.7		1.82	0.28		-3.5	12.7		0.88	0.38	
	MRP2	21.9	11.5		1.8	0.5		40.5	21.5		2.4	0.9		42.3	3.9		2.6	0.2	**
	Control – B	6.2	4.8		1.3	0.2		19.5	7.2		1.8	0.4		17.6	19.1		1.5	0.6	
Pravastatin	BCRP	14.1	15.4		1.30	0.33		17.2	8.0		1.54	0.32		12.1	10.0		1.37	0.32	
	MRP2	-5.7	17.2		0.89	0.32		8.6	27.0		1.18	0.58		15.9	5.6	*	1.68	0.34	
	MRP3	39.5	15.5	**	2.24	0.53	**	32.4	19.9		1.91	0.60		25.0	10.1	*	1.72	0.47	
	MRP4	0.6	11.0		1.02	0.30		13.9	14.9		1.48	0.63		5.2	15.2		1.20	0.67	
	Control	-1.6	7.9		0.95	0.25		5.0	12.4		1.14	0.39		-6.0	9.9		0.88	0.19	
Rosuvastatin	BCRP	343.1	41.4	**	18.49	2.76	**	238.9	17.3	**	15.46	4.08	**	304.7	30.7	**	11.03	1.81	**
	MRP2	-0.6	4.4		0.98	0.14		5.6	5.7		1.33	0.36		7.0	12.1		1.28	0.50	
	MRP4	20.7	10.3		1.98	0.66		25.7	4.2	*	2.84	0.55		22.3	3.5		2.08	0.18	
	MRP8	2.9	16.4		1.08	0.50		4.2	4.7		1.28	0.35		4.7	4.6		1.21	0.25	
	P-gp	3.9	5.0		1.14	0.18		21.7	16.6		1.85	1.14		32.2	9.6		2.47	0.96	
	Control	-2.4	7.9		0.86	0.41		5.6	7.0		1.46	0.61		9.2	7.9		1.47	0.45	

Supplementary table S6: The uptake ratios (the ratio between +ATP and –ATP) and their standard deviation of studied statins in concentration-dependent transport studies at 12 µM statin concentration. N indicates the number of independent experiments carried out with triplicate samples.

Statin	Transporter	Uptake ratio	SD	N
Atorvastatin	BCRP	2.34	0.21	n = 3
Atorvastatin	MRP3	2.44	0.36	n = 3
Atorvastatin	P-gp	3.36	0.24	n = 3
Fluvastatin	BCRP	4.62	0.88	n = 3
Fluvastatin	MRP2	1.81	0.44	n = 3
Fluvastatin	MRP3	2.37	0.38	n = 3
Fluvastatin	MRP4	2.11	0.34	n = 3
Fluvastatin	MRP8	2.02	0.09	n = 3
Fluvastatin	P-gp	2.39	1.09	n = 3
Fluvastatin	Control	1.26	0.15	n = 3
Pitavastatin	BCRP	6.68	1.67	n = 3
Pitavastatin	MRP3	1.75	0.23	n = 3
Pitavastatin	P-gp	2.18	0.28	n = 3
Pitavastatin	Control	0.91	0.17	n = 2
Pravastatin	MRP3	2.19	0.38	n = 4
Rosuvastatin	MRP4	1.95	0.37	n = 3
Rosuvastatin	P-gp	3.01	1.52	n = 3

Supplementary table S7: The transporter abundance in vesicle preparations and protein-specific peptides used in proteomic measurements.

Peptide	Protein-specific peptides	Protein expression$_{\text{in vitro}}$, (pmol/mg of protein)
BCRP	SSLLDVLAAR	146.08
MRP2	LTIIPQDPILFSGSLR	85.33
MRP3	IDGLNVADIGLHDLR	54.24
MRP4	SSLISALFR	43.85
P-gp	AGAVAEEVLAAIR	59.12

Supplementary table S8: The transporter abundance in small intestine and liver according to previous literature and the calculated tissue-specific active efflux clearance values and fractions. The abundance data of Burt et al. 2016 was converted from pmol/10^6 hepatocytes to fmol/mg of tissue according to the hepatocellularity measurements of Sohlenius-Sternbeck 2006[a], where in human 1 g of liver contained 139 x 10^6 hepatocytes.

	Drozdizk et al. 2018 Mean abundance (fmol/mg tissue)			Burt et al. 2016 Mean abundance (fmol/mg of tissue)	Burt et al. 2016 Mean abundance pmol/10^6 hepatocytes
Transporter	Duodenum	Jejunum	Ileum	Liver	Liver
BCRP	5.51	23.27	30.47	8.095	0.058
MRP2	11.88	22.44	19.84	62.865	0.452
MRP3	17.28	30.86	22.58	23.783	0.171
MRP4	13.37	13.87	15.18	7.594	0.055
P-gp	7.67	40.21	70.78	27.816	0.200

Statin	Adj. CL (nL/min/pmol)	CL, duodenum (nL/min/mg tissue)		CL, jejunum (nL/min/mg tissue)		CL, ileum (nL/min/mg tissue)		CL, liver (nL/min/mg tissue)	
Atorvastatin									
BCRP	34.9	0.2	7.1 %	0.7	8.8 %	0.9	7.9 %	0.2	4.5 %
MRP3	140.7	1.2	50.0 %	2.1	26.0 %	1.6	13.1 %	1.6	29.3 %
P-gp	162.9	1.0	42.8 %	5.3	65.3 %	9.4	79.0 %	3.7	66.2 %
Total		2.4	100.0 %	8.2	100.0 %	11.9	100.0 %	5.6	100.0 %
Fluvastatin									
BCRP	338.5	1.6	32.0 %	7.0	52.7 %	9.1	59.6 %	2.4	26.4 %
MRP2	71.3	0.6	11.5 %	1.1	8.5 %	1.0	6.5 %	3.1	34.2 %
MRP3	199.7	1.7	32.8 %	3.0	22.9 %	2.2	14.4 %	2.3	25.3 %
MRP4	122.4	1.0	19.8 %	1.1	8.0 %	1.2	7.6 %	0.6	6.3 %
P-gp	31.7	0.2	3.9 %	1.0	7.9 %	1.8	12.0 %	0.7	7.8 %
Total		5.1	100.0 %	13.2	100.0 %	15.3	100.0 %	9.2	100.0 %
Pitavastatin									
BCRP	156.1	0.8	38.3 %	3.2	50.2 %	4.2	52.0 %	1.1	32.4 %
MRP3	110.8	0.9	47.2 %	1.7	26.2 %	1.2	15.2 %	1.3	37.4 %
P-gp	45.9	0.3	14.5 %	1.5	23.6 %	2.6	32.8 %	1.0	30.2 %
Total		2.0	100.0 %	6.4	100.0 %	8.1	100.0 %	3.4	100.0 %
Rosuvastatin									
BCRP	435.9	2.1	86.8 %	9.0	90.8 %	11.7	88.9 %	3.1	83.8 %
MRP4	22.3	0.2	7.6 %	0.2	2.0 %	0.2	1.6 %	0.1	2.8 %
P-gp	21.8	0.1	5.6 %	0.7	7.2 %	1.3	9.5 %	0.5	13.3 %
Total		2.4	100.0 %	9.9	100.0 %	13.2	100.0 %	3.7	100.0 %

[A]: Sohlenius-Sternbeck A. K. (2006). Determination of the hepatocellularity number for human, dog, rabbit, rat and mouse livers from protein concentration measurements. Toxicology in vitro: an international journal published in association with BIBRA, 20(8), 1582–1586.

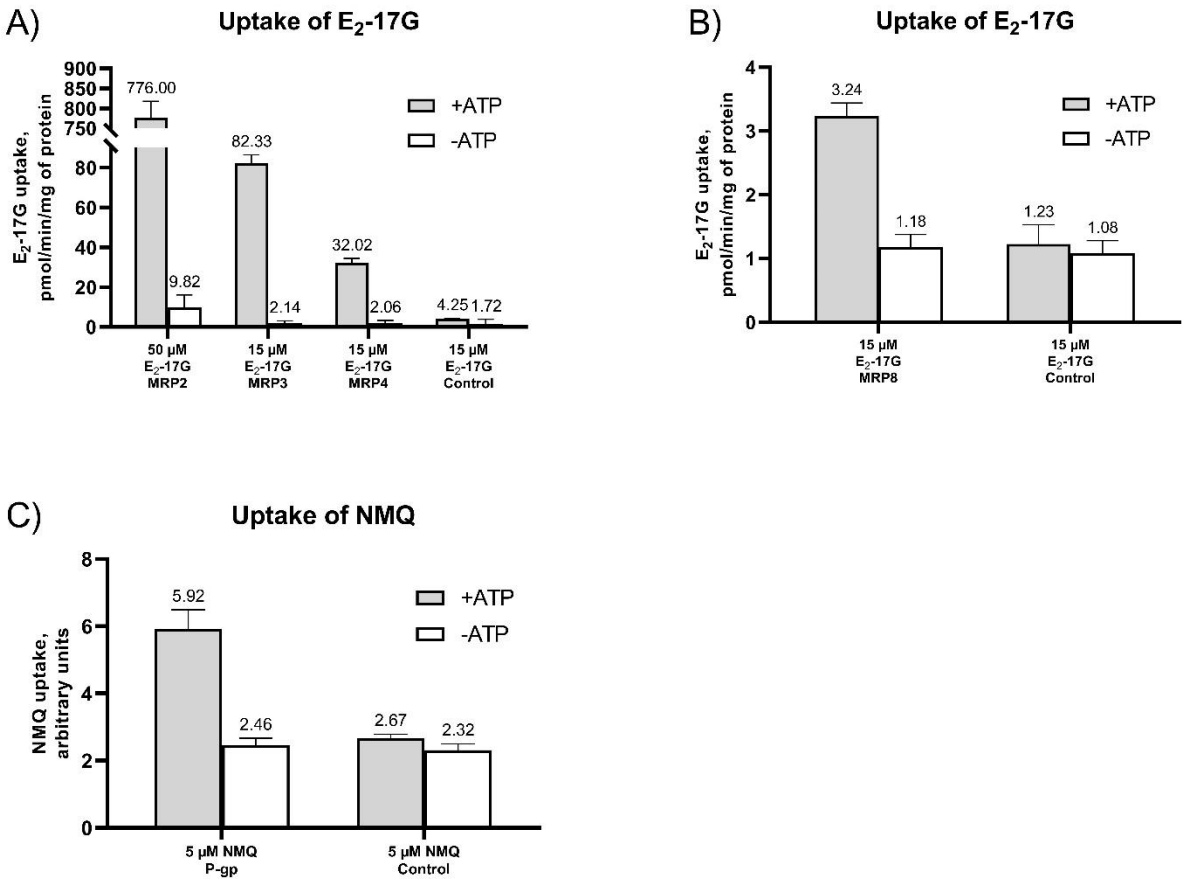

Supplementary figure S1: The transport of estradiol-17-glucuronide (E_2-17G) and N-methyl-quinidine (NMQ) in MRP2, MRP3, MRP4, MRP8, P-gp, and control vesicles. A single transport experiment performed with triplicate samples was conducted to verify the function of each membrane vesicle preparation. The amount of vesicles was 7.5 µg in every experiment. The concentration and incubation time of E_2-17G was 50 µM and 5 min, respectively for MRP2 vesicles, and 10 µM and 10 minutes, respectively, for MRP3, MRP4, MRP8, and control vesicles. The concentration and incubation time of NMQ was 5 µM and 5 min, respectively. A) The uptake of E_2-17G into the MRP2, MRP3, MRP4 and control vesicles in presence (+ATP) and absence (-ATP) of ATP is presented as mean ± SD. B) The uptake of E_2-17G in a separate experiment into the MRP8 and control vesicles in presence (+ATP) and absence (-ATP) of ATP is presented as mean ± SD. C) The uptake of NMQ in into the P-gp and control vesicles in presence (+ATP) and absence (-ATP) of ATP is presented as mean ± SD. Arbitrary units of NMQ uptake stands for the ratio between the peak area of NMQ and internal standard.

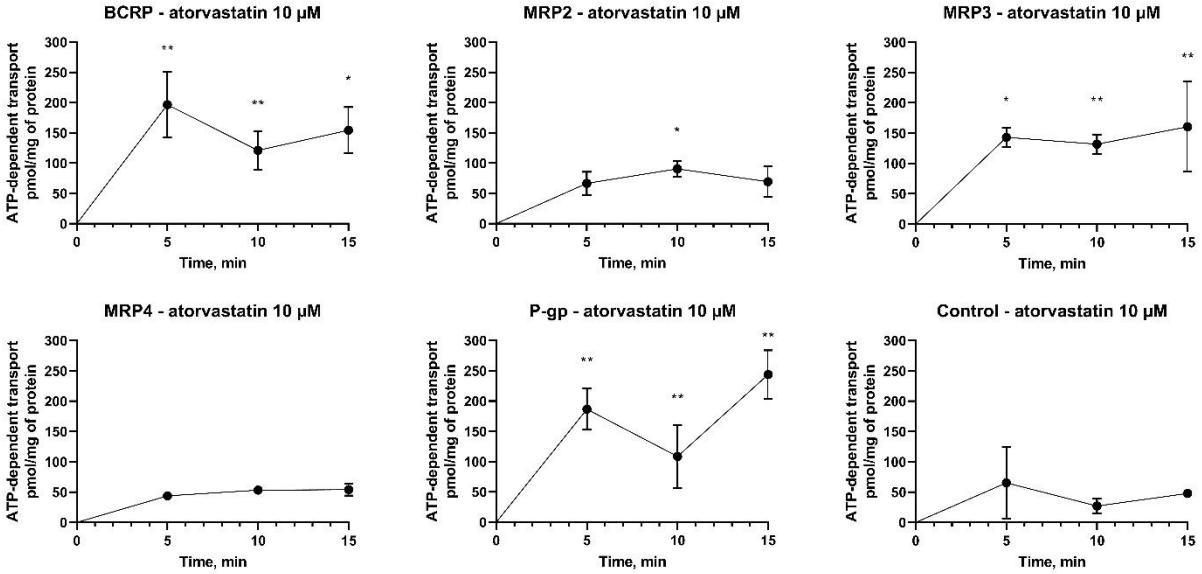

Supplementary figure S2: The time-dependent transport of atorvastatin in BCRP, MRP2, MRP3, MRP4, P-gp, and control vesicles. Substrate concentration, maximum time of incubation, and vesicle amount were 10 µM, 15 min, and 7.5 µg, respectively. Results are presented as mean ± SD ATP-dependent transport obtained from a single experiment, performed with triplicate samples. One-way ANOVA and uncorrected Fisher's LSD analysis were performed to evaluate the transport rate in transporter of interest compared to control. * $p < 0.05$, ** $p < 0.01$.

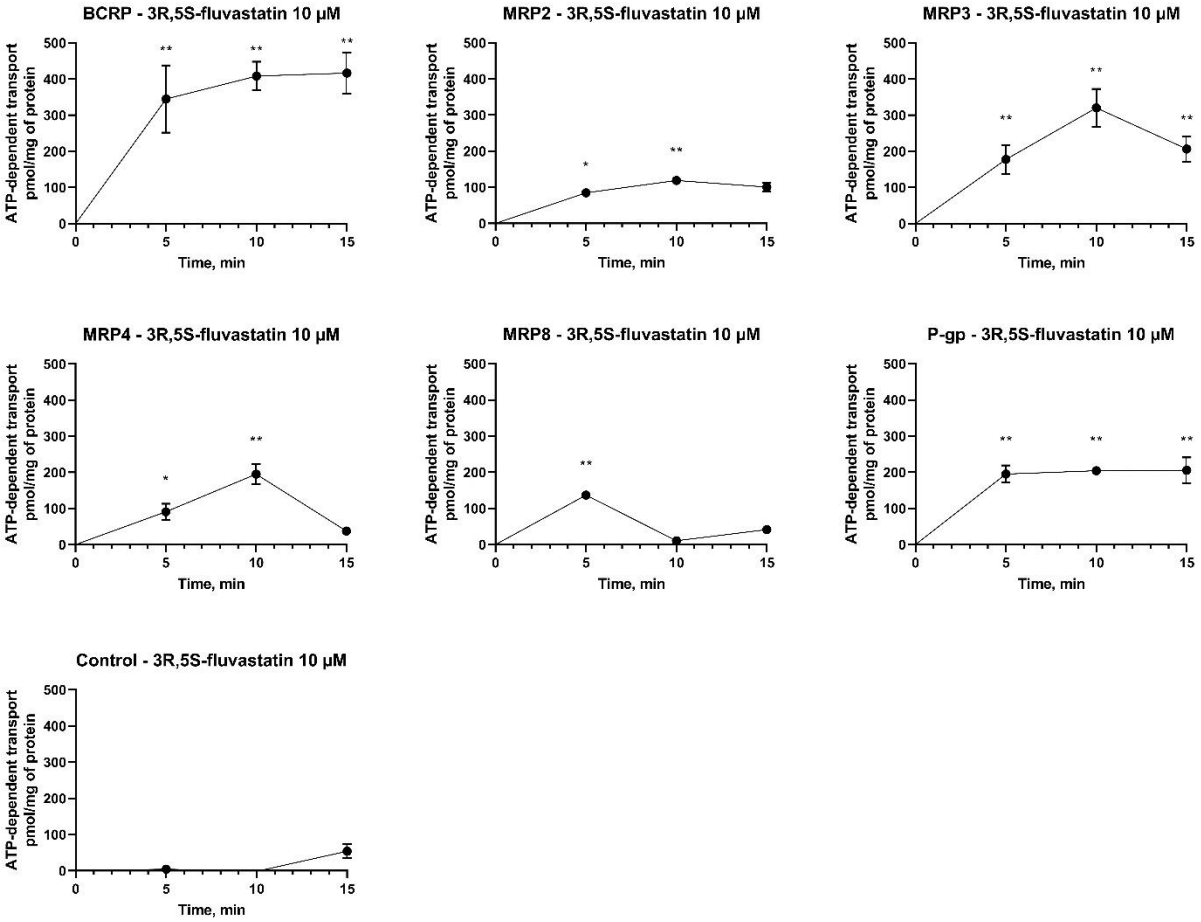

Supplementary figure S3: The time-dependent transport of 3R,5S-fluvastatin in BCRP, MRP2, MRP3, MRP4, MRP8, P-gp, and control vesicles. Substrate concentration, maximum time of incubation, and vesicle amount were 10 µM, 15 min, and 7.5 µg, respectively. Results are presented as mean ± SD ATP-dependent transport obtained from a single experiment, performed with triplicate samples. One-way ANOVA and uncorrected Fisher's LSD analysis were performed to evaluate the transport rate in transporter of interest compared to control. * $p < 0.05$, ** $p < 0.01$.

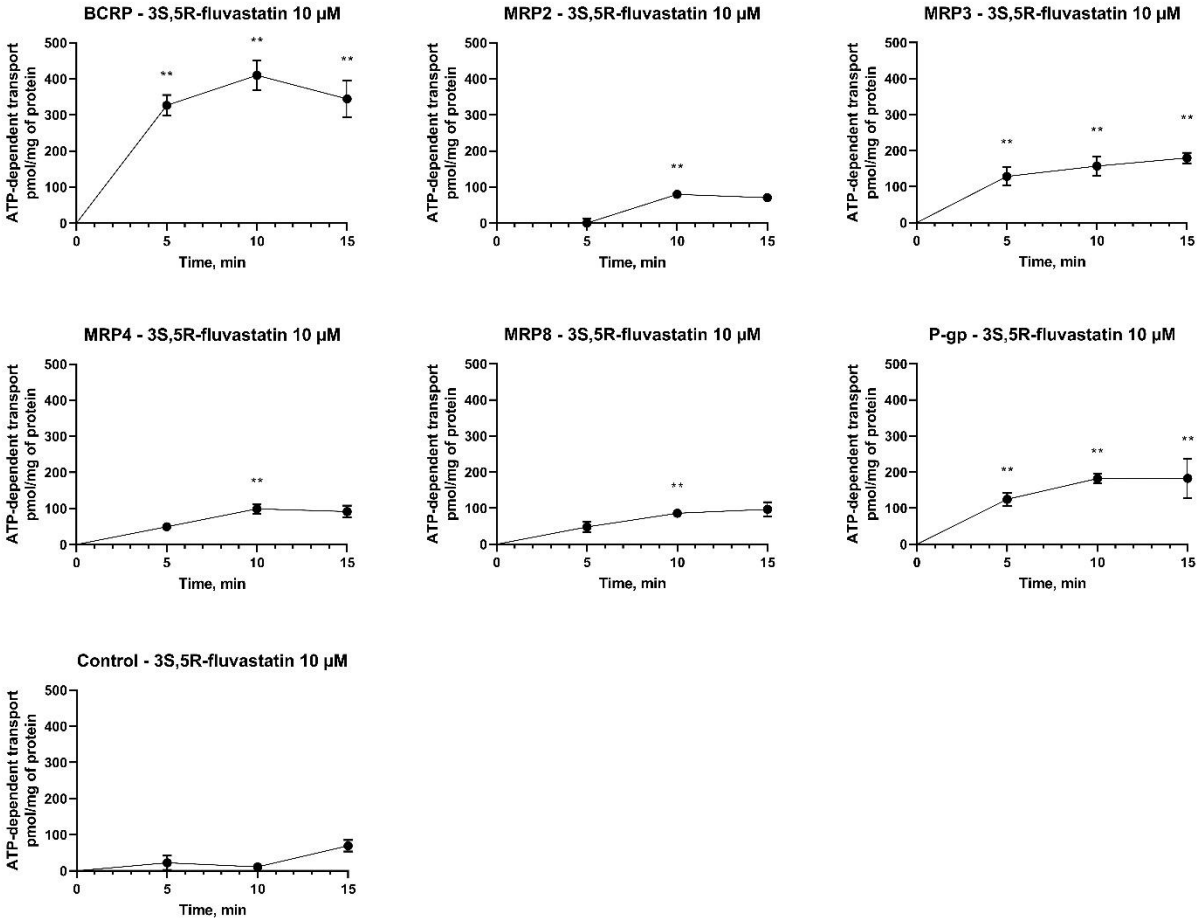

Supplementary figure S4: The time-dependent transport of 3S,5R-fluvastatin in BCRP, MRP2, MRP3, MRP4, MRP8, P-gp, and control vesicles. Substrate concentration, maximum time of incubation, and vesicle amount were 10 µM, 15 min, and 7.5 µg, respectively. Results are presented as mean ± SD ATP-dependent transport obtained from a single experiment, performed with triplicate samples. One-way ANOVA and uncorrected Fisher's LSD analysis were performed to evaluate the transport rate in transporter of interest compared to control. * $p < 0.05$, ** $p < 0.01$.

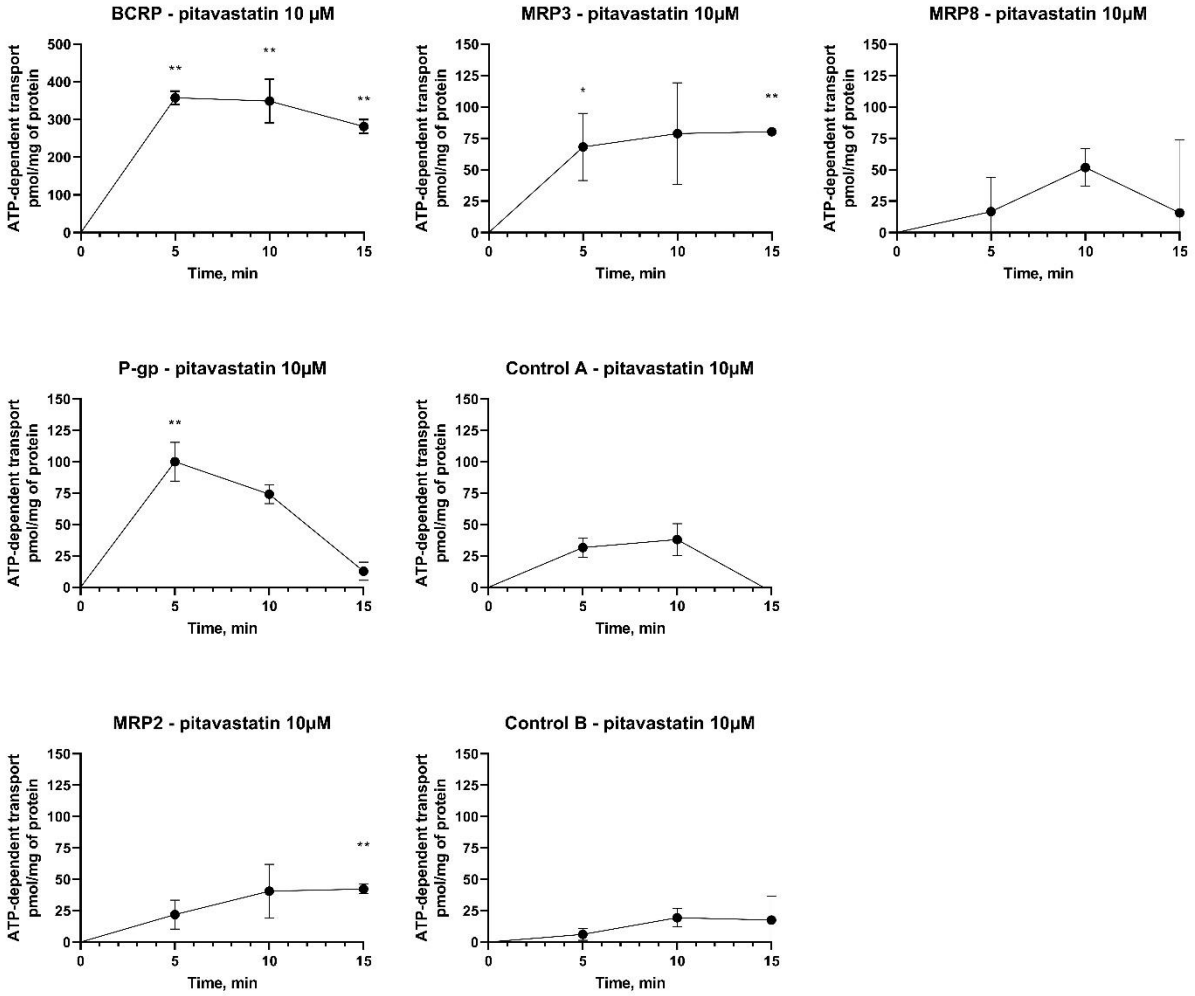

Supplementary figure S5: The time-dependent transport of pitavastatin in BCRP, MRP2, MRP3, MRP8, P-gp, and control vesicles. Substrate concentration, maximum time of incubation, and vesicle amount were 10 µM, 15 min, and 7.5 µg, respectively. Results are presented as mean ± SD ATP-dependent transport obtained from a single experiment, performed with triplicate samples. Note the different y-axis of the BCRP subfigure. One-way ANOVA and uncorrected Fisher's LSD analysis were performed to evaluate the transport rate in transporter of interest compared to control. The transport in BCRP, MRP3, MRP8, and P-gp vesicles was compared to control A, and MRP2 experiment, which was performed on a separate occasion, was compared to control B. * $p < 0.05$, ** $p < 0.01$.

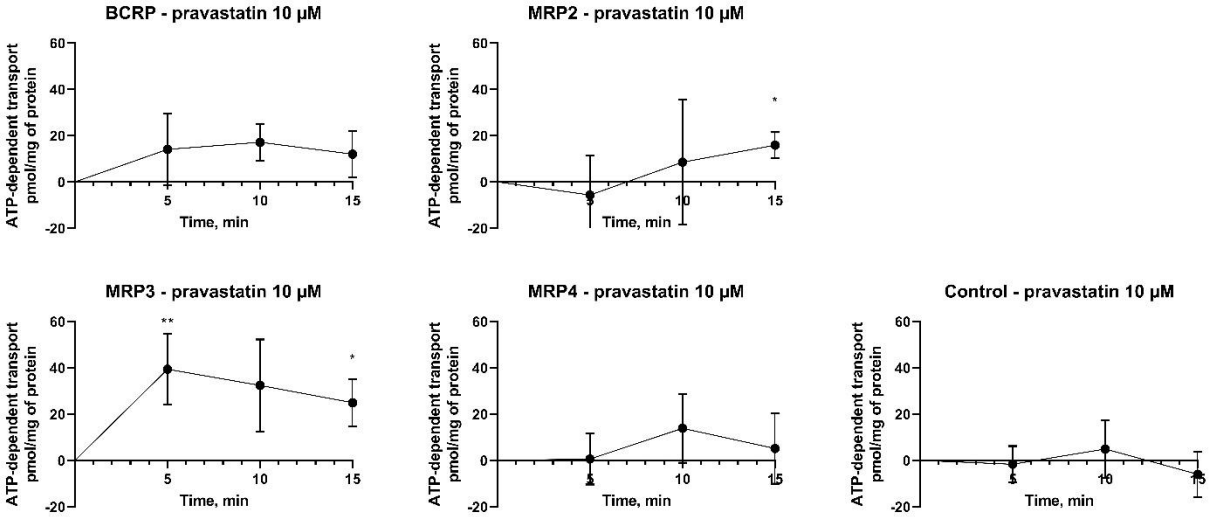

Supplementary figure S6: The time-dependent transport of pravastatin in BCRP, MRP2, MRP3, MRP4, and control vesicles. Substrate concentration, maximum time of incubation, and vesicle amount were 10 µM, 15 min, and 7.5 µg, respectively. Results are presented as mean ± SD ATP-dependent transport obtained from a single experiment, performed with triplicate samples. One-way ANOVA and uncorrected Fisher's LSD analysis were performed to evaluate the transport rate in transporter of interest compared to control. * $p < 0.05$, ** $p < 0.01$

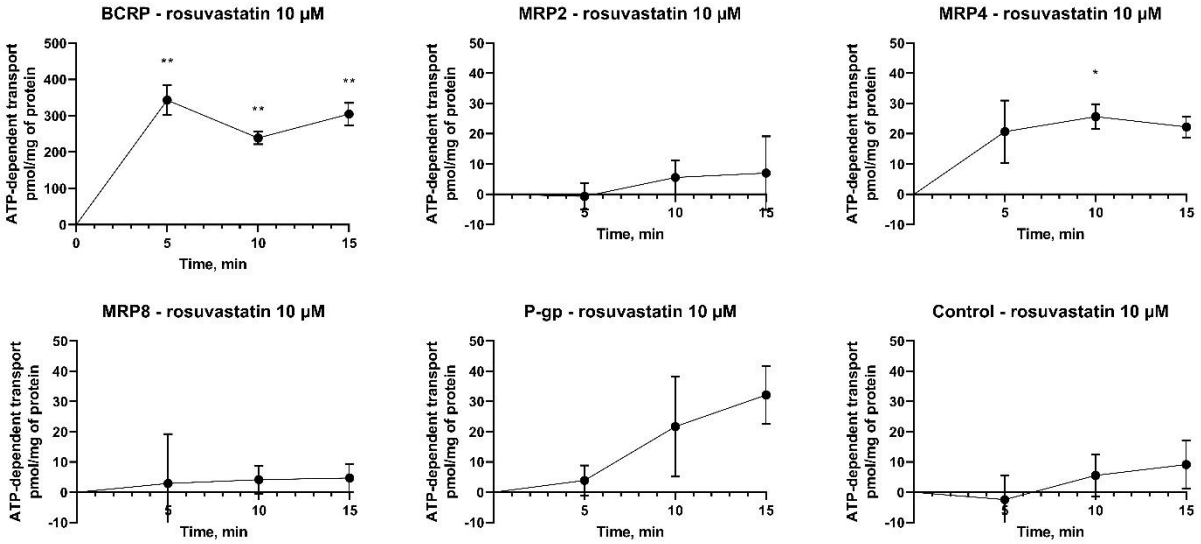

Supplementary figure S7: The time-dependent transport of rosuvastatin in BCRP, MRP2, MRP4, MRP8, P-gp and control vesicles. Substrate concentration, maximum time of incubation, and vesicle amount were 10 µM, 15 min, and 7.5 µg, respectively. Results are presented as mean ± SD ATP-dependent transport obtained from a single experiment, performed with triplicate samples. Note the different y-axis of the BCRP subfigure. One-way ANOVA and uncorrected Fisher's LSD analysis were performed to evaluate the transport rate in transporter of interest compared to control. * $p < 0.05$, ** $p < 0.01$.

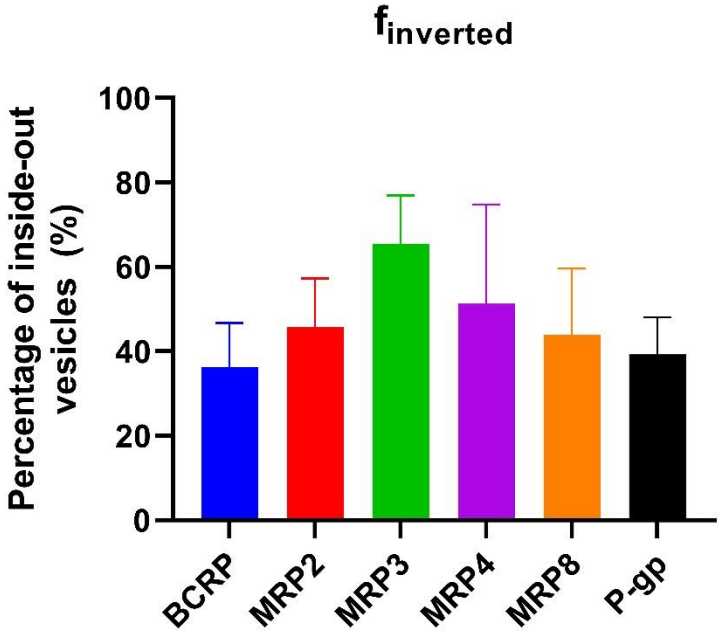

Supplementary figure S8: The fraction of inverted membrane vesicles ($f_{inverted}$) in BCRP, MRP2, MRP4, MRP8, P-gp and control vesicle preparations. Results are presented as mean ± SD obtained from a single experiment, performed with triplicate samples.

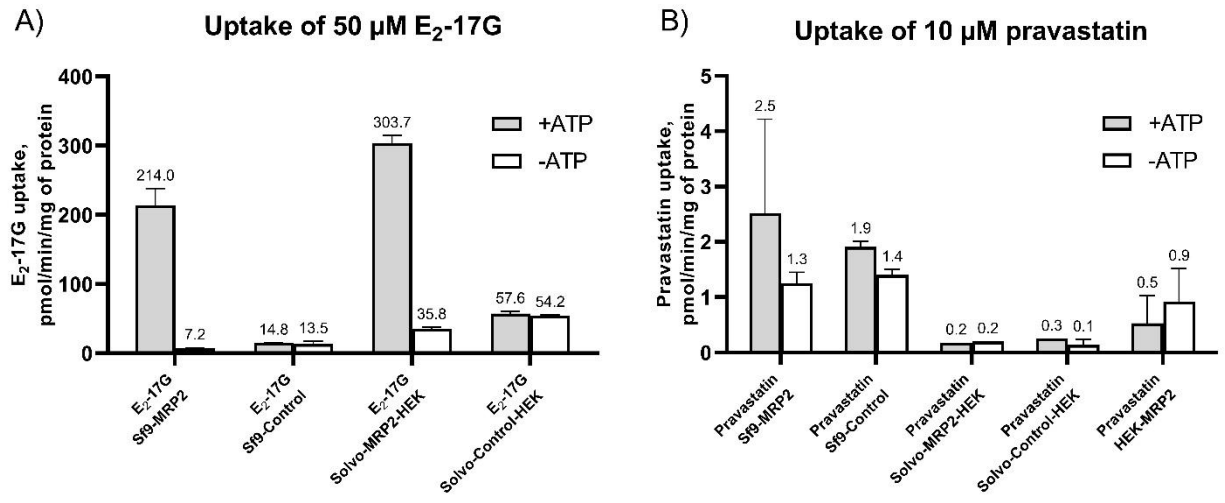

Supplementary figure S9: The transport of 50 µM E_2-17G (panel A) and 10 µM pravastatin (panel B). Compounds of interest were incubated with membrane vesicles supplemented with 3 mM glutathione in the presence and absence of 4 mM ATP for 10 minutes. Sf9 vesicles were generated from the Sf9 insect cells expressing the human recombinant MRP2 or defective mutant of MRP3 (control) (Järvinen et al. 2019[B]). Solvo-MRP2-HEK and Solvo-Control-HEK vesicles were purchased from Solvo Biotechnology (Szeged, Hungary) and HEK-MRP2 from PharmTox at the Radboud University Medical Center (PharmTox, Radboud UMC, Nijmegen, The Netherlands). Results are presented as mean ± SD uptake in the presence (+ATP) and absence (-ATP) of ATP obtained from a single experiment, performed with triplicate samples.

[B]: Järvinen, E., Kidron, H., & Finel, M. (2020). Human efflux transport of testosterone, epitestosterone and other androgen glucuronides. The Journal of steroid biochemistry and molecular biology, 197, 105518.